Table D2.1-4. Model Inputs – Bare Canister

Model Parameter	Value	Basis/Rationale
Canister Properties		
Outer Diameter (m)	1.68	Minimum outer diameter listed in *Transportation, Aging and Disposal Canister System Performance Specification* (Ref. D4.1.28, Section 3.1.1)
Wall Thickness (m)	0.0127 or 0.0254	0.5 inches is the thinnest canister wall thickness listed for current transport cask designs 1.0 inch is the anticipated TAD canister thickness and is also the thickness of the naval SFC
Length (m)	5.4	Typical length of TAD canister listed in *Transportation, Aging and Disposal Canister System Performance Specification* (Ref. D4.1.28, Section 3.1.1)
Density (kg/m^3)	7980	Density of Type 316 stainless steel (Ref. D4.1.7, Table X1.1)
Specific Heat (J/kg K)	560	Approximate value for Type 316 stainless steel at 400C (Ref. D4.1.25, Table 8)
Emissivity	0.8	Estimated value for stainless steel that has undergone some oxidation
Initial Temperature (K)	513	Initial temperature upon removal from the cask. Estimated from *Thermal Responses of TAD and 5-DHLW/DOE SNF Waste Packages to a Hypothetical Fire Accident* (Ref. D4.1.25, Figure 1)
Fuel Properties		
Heated Mass (kg)	9,700	Calculated based on thermal penetration depth (see text)
Specific Heat (J/kg K)	438	Average for fuel region taken from *Thermal Responses of TAD and 5-DHLW/DOE SNF Waste Packages to a Hypothetical Fire Accident* (Ref. D4.1.25, Table 15)
Effective Surface Area (m^2)	28.18	Projected area for radiation heat transfer. Calculated based on outer diameter of fuel region (1.67 m)
Emissivity	0.8	From *Thermal Responses of TAD and 5-DHLW/DOE SNF Waste Packages to a Hypothetical Fire Accident* (Ref. D4.1.25, Table 17)
Initial Temperature (K)	543	Estimated from *Thermal Responses of TAD and 5-DHLW/DOE SNF Waste Packages to a Hypothetical Fire Accident* (Ref. D4.1.25, Figure 1)

Table D2.1-4. Model Inputs – Bare Canister (Continued)

Model Parameter	Value	Basis/Rationale
Post-Fire Conditions		
Ambient Temperature (K)	361	Post-fire temperature of 190°F - a value 100°F higher than the maximum interior facility temperature (Ref. D4.1.16, Section 3.2)
Heat Transfer Coefficient (W/m^2 K)	2.0	Approximate value based on correlations in (Ref. D4.1.41, pp. 456-457) (Results not sensitive to this value)

NOTE: SFC = spent fuel canister; SNF = spent nuclear fuel; TAD = transportation, aging, and disposal.

Source: Original

Table D2.1-5. Model Inputs – Canister in a Waste Package

Model Parameter	Value	Basis/Rationale
Canister Properties		
Outer Diameter (m)	1.68	Minimum diameter listed in *Transportation, Aging and Disposal Canister System Performance Specification* (Ref. D4.1.28, Section 3.1.1)
Wall Thickness (m)	0.0127 or 0.0254	0.5 inches is the thinnest canister wall thickness listed for current transport cask designs 1.0 inch is the anticipated TAD canister thickness and is also the thickness of the naval SFC
Length (m)	5.4	Typical length of TAD canister listed in *Transportation, Aging and Disposal Canister System Performance Specification* (Ref. D4.1.28, Section 3.1.1)
Density (kg/m^3)	7980	Density of Type 316 stainless steel (Ref. D4.1.7, Table X1.1)
Specific Heat (J/kg K)	560	Approximate value for Type 316 stainless steel at 400°C (Ref. D4.1.25, Table 8)
Emissivity	0.62	Average value for Type 316 stainless steel in *Mark's Standard Handbook for Mechanical Engineers* (Ref. D4.1.8, Table 4.3.2)
Initial Temperature (K)	513	From *Thermal Responses of TAD and 5-DHLW/DOE SNF Waste Packages to a Hypothetical Fire Accident* (Ref. D4.1.25, Figure 1)
Outer Barrier of Waste Package		
Outer Diameter (m)	1.8816	Listed in *TAD Waste Package Configuration* (Ref. D4.1.22), (Ref. D4.1.23), and (Ref. D4.1.24)
Wall Thickness (m)	0.0254	Listed in *TAD Waste Package Configuration* (Ref. D4.1.22), (Ref. D4.1.23), and (Ref. D4.1.24)
Length (m)	5.4	Heated length adjacent to the TAD canister – same as TAD canister length
Density (kg/m^3)	8690	Value for Alloy 22 (Ref. D4.1.5, Section II, Part B, SB-575, Section 7.1)
Specific Heat (J/kg K)	476	Value for Alloy 22 at 400°C (Ref. D4.1.36, p. 13)
Emissivity	0.87	Value for Alloy 22 (Ref. D4.1.45, p. 10-297)
Initial Temperature (K)	433	From *Thermal Responses of TAD and 5-DHLW/DOE SNF Waste Packages to a Hypothetical Fire Accident* (Ref. D4.1.25, Figure 1)

Table D2.1-5. Model Inputs – Canister in a Waste Package (Continued)

Model Parameter	Value	Basis/Rationale
Inner Barrier of Waste Package		
Outer Diameter (m)	1.8212	Listed in *TAD Waste Package Configuration* (Ref. D4.1.22), (Ref. D4.1.23), and (Ref. D4.1.24)
Wall Thickness (m)	0.0508	Listed in *TAD Waste Package Configuration* (Ref. D4.1.22), (Ref. D4.1.23), and (Ref. D4.1.24)
Length (m)	5.4	Heated length adjacent to the TAD canister – same as TAD canister length
Specific Heat (J/kg K)	560	Approximate value for Type 316 stainless steel at 400°C (Ref. D4.1.25, Table 8)
Emissivity	0.62	Average value for Type 316 stainless steel in *Mark's Standard Handbook for Mechanical Engineers* (Ref. D4.1.8, Table 4.3.2)
Initial Temperature (K)	478	From *Thermal Responses of TAD and 5-DHLW/DOE SNF Waste Packages to a Hypothetical Fire Accident* (Ref. D4.1.25, Figure 1)
Post-Fire Conditions		
Ambient Temperature (K)	361	Post-fire temperature of 190°F - a value 100°F higher than the maximum interior facility temperature (Ref. D4.1.16, Section 3.2)
Heat Transfer Coefficient (W/m^2 K)	2.0	Approximate value based on correlations in *Introduction to Heat Transfer* (Ref. D4.1.41, pp. 456-457) (Results not sensitive to this value)

NOTE: SFC = spent fuel canister; SNF = spent nuclear fuel; TAD = transportation, aging, and disposal.

Source: Original

Table D2.1-6. Model Inputs – Canister in Transportation Cask

Model Parameter	Value	Basis/Rationale
Canister Properties		
Outer Diameter (m)	1.68	Minimum diameter listed in *Transportation, Aging and Disposal Canister System Performance Specification* (Ref. D4.1.28, Section 3.1.1)
Wall Thickness (m)	0.0127 or 0.0254	0.5 inches is the thinnest canister wall thickness listed for current transport cask designs 1.0 inch is the anticipated TAD canister thickness and is also the thickness of the naval SFC
Length (m)	5.4	Typical length of TAD canister listed in *Transportation, Aging and Disposal Canister System Performance Specification* (Ref. D4.1.28, Section 3.1.1)
Density (kg/m^3)	7980	Density of Type 316 stainless steel (Ref. D4.1.7, Table X1.1)
Specific Heat (J/kg K)	560	Approximate value for Type 316 stainless steel at 400°C (Ref. D4.1.25, Table 8)
Emissivity	0.62	Average value for Type 316 stainless steel in *Mark's Standard Handbook for Mechanical Engineers* (Ref. D4.1.8, Table 4.3.2)
Initial Temperature (K)	513	From *Thermal Responses of TAD and 5-DHLW/DOE SNF Waste Packages to a Hypothetical Fire Accident* (Ref. D4.1.25, Figure 1)
Transportation Cask Outer Shell		
Outer Diameter (m)	2.438	From HI-STAR Transportation Cask SAR (Ref. D4.1.38, p. 1.2-3)
Wall Thickness (m)	0.0127	Minimum outer shell thickness listed in cask SARs
Length (m)	5.4	Length adjacent to the TAD canister
Density (kg/m^3)	7850	Density of 516 carbon steel (Ref. D4.1.6, Section II, Part A, SA-20, 14.1)
Specific Heat (J/kg K)	604	Approximate value for 516 carbon steel at 400°C (Ref. D4.1.25, Table 10)
Emissivity	0.8	Average value for carbon steel in *Mark's Standard Handbook for Mechanical Engineers* (Ref. D4.1.8, Table 4.3.2)
Initial Temperature (K)	381	Initial temperature in HI-STAR SAR (Ref. D4.1.38, Figure 3.5.3)

Table D2.1-6. Model Inputs – Canister in Transportation Cask (Continued)

Model Parameter	Value	Basis/Rationale
Transportation Cask Gamma Shield		
Outer Diameter (m)	2.148	From HI-STAR Transportation Cask SAR (Ref. D4.1.38, Drawing No.3913)
Wall Thickness (m)	0.19	A lower value for the combined thickness of gamma shield and inner containment listed in cask SARs
Length (m)	5.4	Length adjacent to the TAD canister
Density (kg/m^3)	7850	Density of 516 carbon steel (Ref. D4.1.6, Section II, Part A, SA-20, 14.1)
Specific Heat (J/kg K)	604	Approximate value for 516 carbon steel at 400°C (Ref. D4.1.25, Table 10)
Emissivity	0.8	Average value for carbon steel in *Mark's Standard Handbook for Mechanical Engineers* (Ref. D4.1.8, Table 4.3.2)
Initial Temperature (K)	405	Approximate average initial temperature in HI-STAR SAR (Ref. D4.1.38, Figure 3.5.3)
Ambient Temperature (K)	361	Post-fire temperature of 190°F - a value 100°F higher than the maximum interior facility temperature (Ref. D4.1.16, Section 3.2)
Heat Transfer Coefficient (W/m^2 K)	2.0	Approximate value based on correlations in *Introduction to Heat Transfer* (Ref. D4.1.41, pp. 456-457) (Results not sensitive to this value)

NOTE: SAR = Safety Analysis Report; SFC = spent fuel canister; SNF = spent nuclear fuel; TAD = transportation, aging, and disposal.

Source: Original

Table D2.1-7. Model Inputs – Canister in a Shielded Bell

Model Parameter	Value	Basis/Rationale
Canister Properties		
Outer Diameter (m)	1.68	Minimum diameter listed in *Transportation, Aging and Disposal Canister System Performance Specification* (Ref. D4.1.28, Section 3.1.1)
Wall Thickness (m)	0.0127 or 0.0254	0.5 inches is the thinnest canister wall thickness listed for current transport cask designs 1.0 inch is the anticipated TAD canister thickness and is also the thickness of the naval SFC
Length (m)	5.4	Typical length of TAD canister listed in *Transportation, Aging and Disposal Canister System Performance Specification* (Ref. D4.1.28, Section 3.1.1)
Density (kg/m^3)	7980	Density of Type 316 stainless steel (Ref. D4.1.7, Table X1.1)
Specific Heat (J/kg K)	560	Approximate value for Type 316 stainless steel at 400°C (Ref. D4.1.25, Table 8)
Emissivity	0.62	Average value for Type 316 stainless steel in *Mark's Standard Handbook for Mechanical Engineers* (Ref. D4.1.8, Table 4.3.2)
Initial Temperature (K)	513	From *Thermal Responses of TAD and 5-DHLW/DOE SNF Waste Packages to a Hypothetical Fire Accident* (Ref. D4.1.25, Figure 1)
Shielded Bell		
Outer Diameter (m)	2.388	From *CRCF, IHF, RF, and WHF Canister Transfer Machine Mechanical Equipment Envelope* (Ref. D4.1.11)
Wall Thickness (m)	0.273	From *CRCF, IHF, RF, and WHF Canister Transfer Machine Mechanical Equipment Envelope* (Ref. D4.1.11)
Length (m)	7.62	From *CRCF, IHF, RF, and WHF Canister Transfer Machine Mechanical Equipment Envelope* (Ref. D4.1.11)
Density (kg/m^3)	7980	Density of Type 316 stainless steel (Ref. D4.1.7, Table X1.1)
Specific Heat (J/kg K)	560	Approximate value for Type 316 stainless steel at 400°C (Ref. D4.1.25, Table 8)
Emissivity	0.67	Approximate value at elevated temperature (corresponds to little oxidation of the surface)
Initial Temperature (K)	306	Maximum interior facility temperature of 90°F (Ref. D4.1.16, Section 3.2)
Post-Fire Conditions		
Ambient Temperature (K)	367	Post-fire temperature of 190°F - a value 100°F higher than the maximum operating temperature listed above
Heat Transfer Coefficient (W/m^2 K)	2.0	Approximate value based on correlations in *Introduction to Heat Transfer* (Ref. D4.1.41, pp. 456-457) (Results not sensitive to this value)

NOTE: SFC = spent fuel canister; SNF = spent nuclear fuel; TAD = transportation, aging, and disposal.

Source: Original

D2.1.4.5 Uncertainty in Canister Failure Temperature

Using the models discussed in Sections D2.1.4.1 and D2.1.4.2, the temperature increase of a canister due to a fire can be calculated. In order to determine whether the temperature is sufficient to cause the canister to fail, it is necessary to determine the canister temperature at which failure would occur. Two failure modes were considered:

1. *Creep-Induced Failure.* Creep is the plastic deformation that takes place when a material is held at high temperature for an extended period under tensile load. This mode of failure is possible for long duration fires.

2. *Limit Load Failure.* This failure mode occurs when the load exerted on a material exceeds its structural strength. As the temperature of the canister increases in temperature, its strength decreases. Failure is generally predicted at some fraction (usually around 70%) of the ultimate strength.

The modeling associated with these failure modes is described in the following subsections.

D2.1.4.5.1 Modeling Creep-Induced Failure

Creep failure could occur if the canister is maintained at a high temperature for a lengthy period of time. One way to predict creep failure is to calculate a creep damage index, which defines the ratio of the creep damage to the cumulative creep required for failure. Such a model has been used by researchers at Argonne National Laboratory to predict failure of steam generator tubes under accident conditions (Ref. D4.1.46). In the Argonne National Laboratory model, failure occurs when the creep damage index reaches a value of 1. Written in the form of an equation, this condition is given by Equation D-16:

$$\int_0^{t_f} \frac{dt}{t_R(T,\sigma)} = 1 \qquad \text{(Eq. D-16)}$$

where

T = the temperature experienced by the canister (a function of time)

σ = the tensile stress exerted on the canister wall

t_f = the canister failure time (the time at which the equality is satisfied).

The function in the denominator of Equation D-16 is Equation D-17:

$$t_R = 10^{\frac{P_{LM}}{T} - 20} \qquad \text{(Eq. D-17)}$$

where P_{LM} is the Larson-Miller parameter (Ref. D4.1.44), which is a material property of the canister material and is a function of the applied stress.

Since the canisters are pressurized to varying degrees with a combination of helium or air used to backfill the canister and gases released when the fuel fails, the pressure inside the canister will increase as the canister gets hotter. The internal pressure exerts a hoop stress in the radial direction that puts the canister wall under tension. It is this stress that controls failure of the canister wall. The hoop stress, σ, is calculated using the following Equation D-18:

$$\sigma = \frac{P r_c}{h} \qquad \text{(Eq. D-18)}$$

where

h	=	the thickness of the canister wall
r_c	=	the mean radius of the canister
P	=	the pressure difference across the canister wall.

D2.1.4.5.2 Modeling Limit Load Failure

Limit load failure occurs when the load on a structure exceeds its ability to withstand that load. As with the creep failure mode, the load on the canister wall is a hoop stress and is calculated using Equation D-18.

The capability of the canister to withstand a load is given by a flow stress, which is defined by (Ref. D4.1.46, p. 3) Equation D-19:

$$\overline{\sigma} = k(\sigma_y + \sigma_u) \qquad \text{(Eq. D-19)}$$

where

k	=	a multiplication factor (0.5 in the current analysis)
σ_y	=	the yield strength (temperature dependent)
σ_u	=	the ultimate strength (temperature dependent).

The yield and ultimate strength are both temperature-dependent properties, so the flow stress is also a temperature-dependent property. For a typical 316 stainless steel, a value of 0.5 for k yields a flow stress that is approximately 0.7 times the ultimate strength. Failure is predicted if the hoop stress exceeds the flow stress.

This failure condition is consistent with the failure condition outlined in *2004 ASME Boiler and Pressure Vessel Code* (Ref. D4.1.6, Appendix F, paragraph F-1331). The American Society of Mechanical Engineers (ASME) code specifies that for ferritic steels, the primary membrane stress intensity shall not exceed 0.7 σ_u. For austenitic steels, the primary membrane stress intensity shall not exceed the greater of 0.7 σ_u or $\sigma_y + (\sigma_u + \sigma_y)/3$. As is noted below, for type 316 stainless steels, 0.7 σ_u is always the controlling condition.

D2.1.4.5.3 Inputs to the Canister Failure Models

The canister failure models require the following inputs:

- the value for the Larson-Miller parameter (a function of temperature and stress)
- the value for the flow stress (a function of temperature)
- the time-dependent internal pressure and temperature experienced by the canister.

The following discussion outlines how these values were determined.

D2.1.4.5.3.1 Larson-Miller Parameter

The value for the Larson-Miller parameter can be determined based on creep data provided by material suppliers. In the absence of data specific to the steels used for the spent fuel and high level waste canisters to arrive at Yucca Mountain, a literature review was performed to obtain representative creep rupture data for steels of the type expected to be used.

The primary focus of this data search was type 316 stainless steel since that is the steel most likely to be used for the spent fuel or high level waste canisters. Data were collected from the following sources:

- "Properties and Selection of Metals." Volume 1 of *Metals Handbook* (Ref. D4.1.3).
- Reliability and Longevity of Furnace Components as Influenced by Alloy of Construction. H-3124 (Ref. D4.1.35).
- *Creep of the Austenitic Steel AISI 316L(N) -Experiments and Models* (Ref. D4.1.58).
- Assessment of Creep Behaviour of Austenitic Stainless Steel Welds (Ref. D4.1.59).
- *Materials Selection for High Temperature Applications* (Ref. D4.1.60).

The creep data provides the time required for creep rupture given a specified constant temperature and applied tensile stress.

Using this data, the value for the Larson-Miller parameter (Ref. D4.1.44) can be determined from the following Equation D-20:

$$P_{LM} = T[C + \log(t_f)] \qquad \text{(Eq. D-20)}$$

where

T	=	temperature (K)
t_f	=	failure time (hours) determined in testing
C	=	a constant that is approximately 20 for most stainless steels

Using this equation and the data collected in the literature review, values for the Larson-Miller parameter were calculated. The calculated values for the Larson-Miller parameter are shown in Figure D2.1-2. As shown in the figure, the Larson-Miller parameter decreases as the applied stress increases.

In order to apply the results shown in the table outside the range of stresses considered in the table, it is necessary to determine a correlation that best fits the data. The best-fit curve, which is also plotted in Figure D2.1-2, is given by the following Equation D-21:

$$P_{LM} = 33{,}845 - 2{,}423\ln(\sigma) \qquad \text{(Eq. D-21)}$$

As shown in Figure D2.1-2, the value for the Larson-Miller parameter varies from one metal specimen to the next and from one vendor to the next. This variability is illustrated, in part, by the variability in the data shown in the figure. In addition, the research by Sasikala, et al. (Ref. D4.1.59) showed that stainless steel weld material is generally less creep-resistant than the base metal (this is illustrated by the five outlier points on the figure which were determined for the weld material rather than the base metal). The variability in the Larson-Miller parameter must be reflected in the uncertainty analysis for the canister failure temperature.

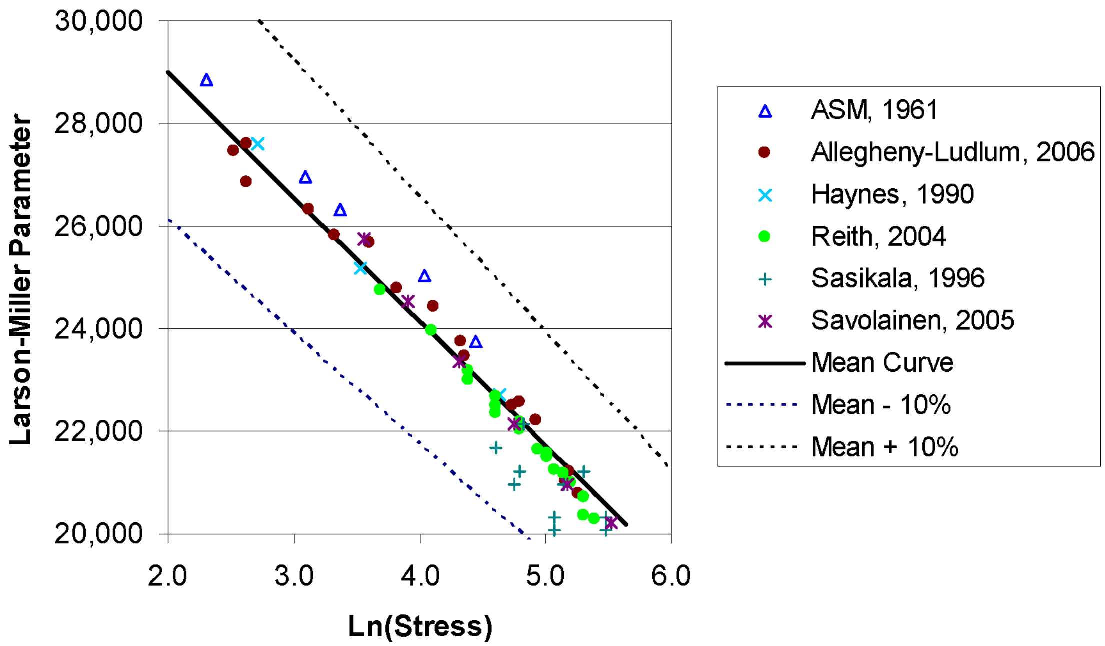

Source: Excel Spreadsheet *Creep rupture - Fast Heatup 1 inch.xls* found in Attachment H

Figure D2.1-2. Plot of Larson-Miller Parameter for Type 316 Stainless Steel

The uncertainty in the Larson-Miller parameter is treated within the canister failure analysis by multiplying the calculated value for P_{LM} by a factor (1+a), where the value for *a* is normally distributed with a mean of 0.0 and a standard deviation of 0.038. Using this formulation, 99% of all canister steels would have P_{LM} values within approximately 10 % of the calculated value.

This uncertainty is believed to reflect the variability between different canister steels as well as the variability between the base metal and the weld material.

D2.1.4.5.3.2 Flow Stress

In the canister failure analysis, the flow stress is the average of the yield and ultimate strength. Both the yield and ultimate strength are temperature-dependent and decrease rapidly above a temperature of about 800°K. Figure D2.1-3 presents typical curves for the yield and ultimate strength of Type 316 stainless steel as a function of temperature (Ref. D4.1.1). The figure also presents the calculated flow stress curve. For temperatures with no yield strength data, the flow stress equals 0.7 times the ultimate strength.

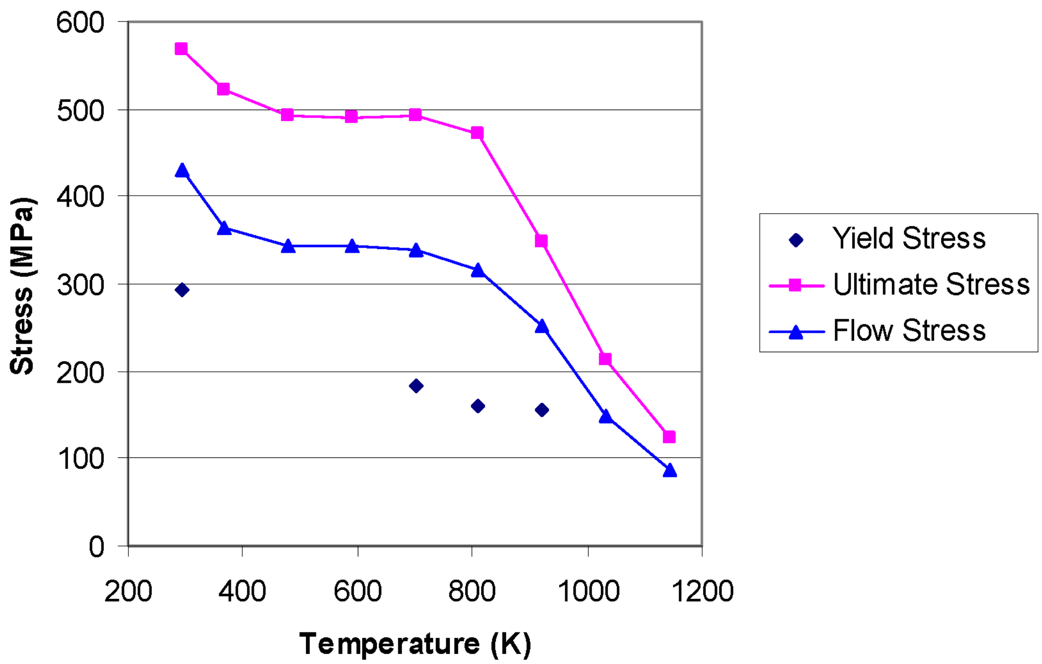

NOTE: K = Kelvin; MPa = megapascals.

Source: Original

Figure D2.1-3. Yield, Ultimate, and Flow Stress for Type 316 Stainless Steel

For the temperature range of interest, the flow stress curve can be fit to two straight lines: one line for temperatures between 350°K and 800°K and another for temperatures above 800°K. The equations for these two lines are provided below (Equations D-22a and D-22b):

$$\overline{\sigma} = 395.9 - 0.0925T \quad \text{for } T < 800\text{ K} \quad (R^2 = 0.889) \qquad \text{(Eq. D-22a)}$$

$$\overline{\sigma} = 899.1 - 0.7139T \quad \text{for } T \geq 800\text{ K} \quad (R^2 = 0.989) \qquad \text{(Eq. D-22b)}$$

Note that the fit is particularly good for the upper temperature range, which is of greatest interest in the current analysis.

As with the value for the Larson-Miller parameter, the value for the flow stress is uncertain. The uncertainty in the flow stress was treated in the same manner at the uncertainty in the Larson-Miller parameter. Specifically, the mean value described by the equations provided above was multiplied by a factor (1 + a) where the value for *a* is normally distributed with a standard deviation of 0.038. This distribution results in 99 % of all canister steels having a flow stress within 10 % of the mean value given by the equations. This adequately reflects the variability in the material properties of Type 316 steels, the variability between the properties of the base metal and weld material, and the potential for other types of steel with lower or higher tensile strength to be used in manufacture of the canisters.

D2.1.4.5.3.3 Pressure Difference and Temperature Histories

Creep failure and limit load failure depend on the time-dependent internal pressure and canister temperature. The canister temperature depends on the fire severity and also on whether the canister is bare or enclosed in a waste package or cask. The canister temperature is calculated using a separate analysis, as discussed above. Rather than attempting to couple the canister failure and canister heatup analyses into a single calculation, a separate canister failure analysis was completed. This analysis required the following inputs: the rate of temperature increase of the canister wall and the relationship between the internal canister pressure and the temperature of the canister wall.

Based on a series of runs with the canister heat transfer models discussed above, it was determined that the rate of temperature increase for a bare canister was likely to range from a low of around 25°K/min to a high of around 175°K/min. This range was input as a normal distribution with a mean of 100°K/min and a standard deviation of 25°K/min. Similar runs for the non-bare canister cases indicated a much slower heatup rate. For these cases, the canister heatup rate was input as a normal distribution with a mean of 10°K/min and a standard deviation of 2.5°K/min.

Analyses with a special version of the bare canister heat transfer model were also used to characterize the rate at which the temperature of the gas inside the canister would increase as a result of heating of the canister wall. This version of the model included convective heat transfer from the canister wall to the gas, from the canister wall to fuel assemblies inside the canister, and from the fuel assemblies to the gas inside the canister. These analyses showed a substantial lag in temperature between the canister wall and the gas.

The following equation was used to calculate the internal pressure of the canister based on the canister temperature (Equation D-23):

$$P = P_0 \left[1 + C\left(\frac{T_{can} - T_{can,0}}{T_{can,0}}\right) \right] \qquad \text{(Eq. D-23)}$$

where

P_0	=	initial pressure inside the canister (including potential fuel failures)
$T_{can,0}$	=	initial temperature of the canister wall
T_{can}	=	canister temperature at the current timestep
C	=	a constant that depends on the canister heating rate.

Note that if the value for C is set equal to 1.0 in this equation, the proportional change in pressure is equal to the proportional change in temperature. This would be true if the gas and canister temperatures increased at the same rate. Because the gas temperature lags behind the canister temperature, the value for C is always less than 1. Rather than attempting to model the variability in the value for C, the analysis used a bounding value of 0.5 for all analyses. This value bounded the range of values calculated in the separate heat transfer analysis.

The initial pressure, P_0, in Equation D-23 varies over a wide range depending on the amount of overpressure supplied when the canister is sealed, the extent of fuel rod failures, and the type of fuel stored in the canister. Since the canister failure analysis considers only the increase in gas temperature due to the fire, the initial pressure must reflect potential fuel failures during the fire.

The SARs prepared by transportation cask vendors were consulted for information on internal pressure under normal and accident conditions (see for example, Section 3.6.6 of *GA-9 Legal Weight Truck From-Reactor Spent Fuel Shipping Cask, Final Design Report* (Ref. D4.1.34)). The SARs provide information on the initial overpressure in the canister and the pressure increase associated with fuel rod failures. Based on this information, an uncertainty distribution for the initial pressure in the canister was developed. The uncertainty is characterized by a Weibull distribution with a minimum of 5 psig, a scale factor of 45 psig, and a shape factor of 2.4. This distribution is applied to all canisters considered in the PCSA.

D2.1.5 Probabilistic Fragility Analysis

The mechanistic models described above produce results that are deterministic. That is, for a given set of input values, they yield a single answer. However, as has been shown, the inputs to the models are uncertain. Uncertainty in the input parameters could lead to a substantial variation in the predicted canister thermal response and failure temperature. Therefore, it is necessary to treat the analysis in a probabilistic manner. It is in the fragility analysis that all the parameters that affect the failure of the spent fuel or high level waste canister are addressed in a probabilistic fashion.

The fragility analysis consists of two separate probabilistic analyses: (1) an analysis to determine the probability distribution for the canister failure temperature, and (2) an analysis to determine the maximum temperature reached by the canister due to the fire. These two analyses are combined to determine the probability that the canister fails as a result of the fire.

Calculations were performed for canisters inside a waste package, a cask, or a shielded bell. As discussed earlier, two canister wall thicknesses were evaluated: 0.5 inches (hereafter referred to as *thin-walled* canisters) and 1.0 inch (hereafter referred to as *thick-walled* canisters). The following sections describe how these analyses are performed and present the calculated failure probabilities for the various canister configurations of interest.

D2.1.5.1 Probabilistic Analysis of Canister Failure Temperature

The first step in the fragility analysis was to determine the probability distribution for the canister failure temperature. The probability distribution was determined using a Monte Carlo analysis in which the failure models outlined in Section D2.1.4 were repeatedly solved with parameter values sampled from the uncertainty distributions discussed in that section. The failure temperature for each sample was the lower of the two temperatures calculated based on creep rupture or limit load failure.

A Microsoft Excel add-in product, Crystal Ball, was used to perform Monte Carlo simulation. Latin hypercube sampling was used to ensure that parameter samples represented the assigned distributions adequately.

Figure D2.1-4 shows the calculated canister failure temperature distribution for canisters inside a waste package, transportation cask, or shielded bell. This calculation used the lower heating rate discussed in Section D2.1.4.5.3.3. The probability distribution shown in Figure D2.1-4 is well-characterized by a normal distribution with a mean of 1,203°K and a standard deviation of 22.85°K. This normal distribution provides a particularly good fit to the lower failure temperature portion of the distribution which is the most important for the canister failure analysis.

A similar analysis was performed for bare canisters. This calculation used the higher heating rate discussed in Section D2.1.4.5.3.3. The resulting probability distribution was nearly identical to the one shown in Figure D2.1-4. The reason for this is that canister failure was nearly always due to limit load failure rather than creep failure, so the difference in heating rates for the two configurations was not important.

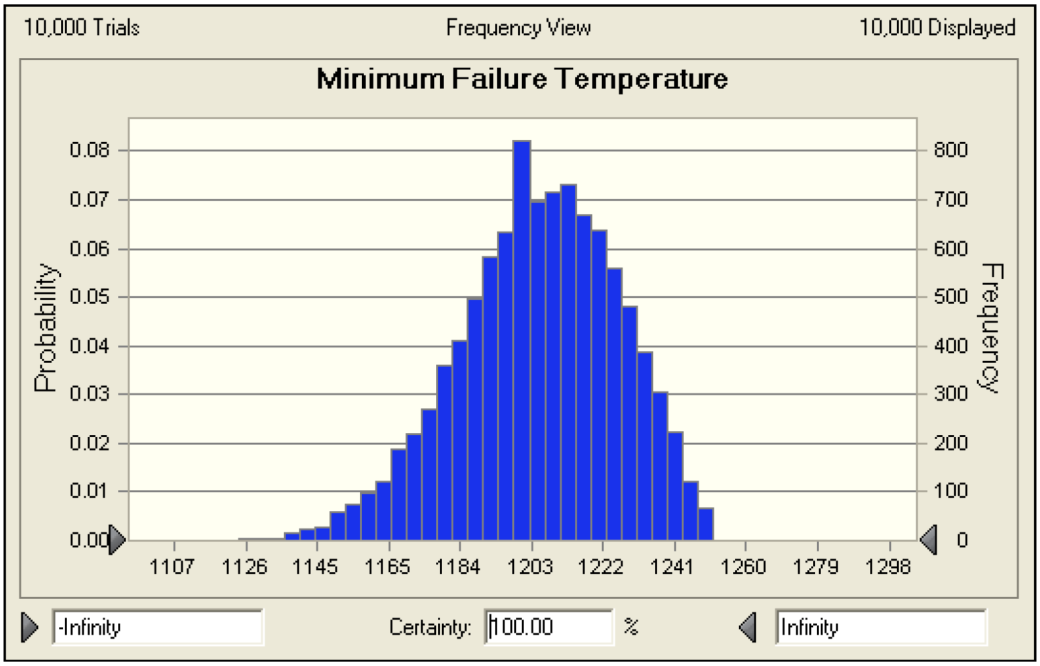

Source: Original

Figure D2.1-4. Probability Distribution for the Failure Temperature of Thin-Walled Canisters

A similar analysis was performed for thick-walled canisters. As with the thin-walled canisters, the probability distribution for the canister failure temperature was found to be nearly independent of the canister heating rate. Figure D2.1-5 shows the calculated probability distribution. This probability distribution is well-characterized by a normal distribution with a mean of 1,232°K and a standard deviation of 12.3°K. This normal distribution provides a particularly good fit to the lower failure temperature portion of the distribution which is the most important for the canister failure analysis.

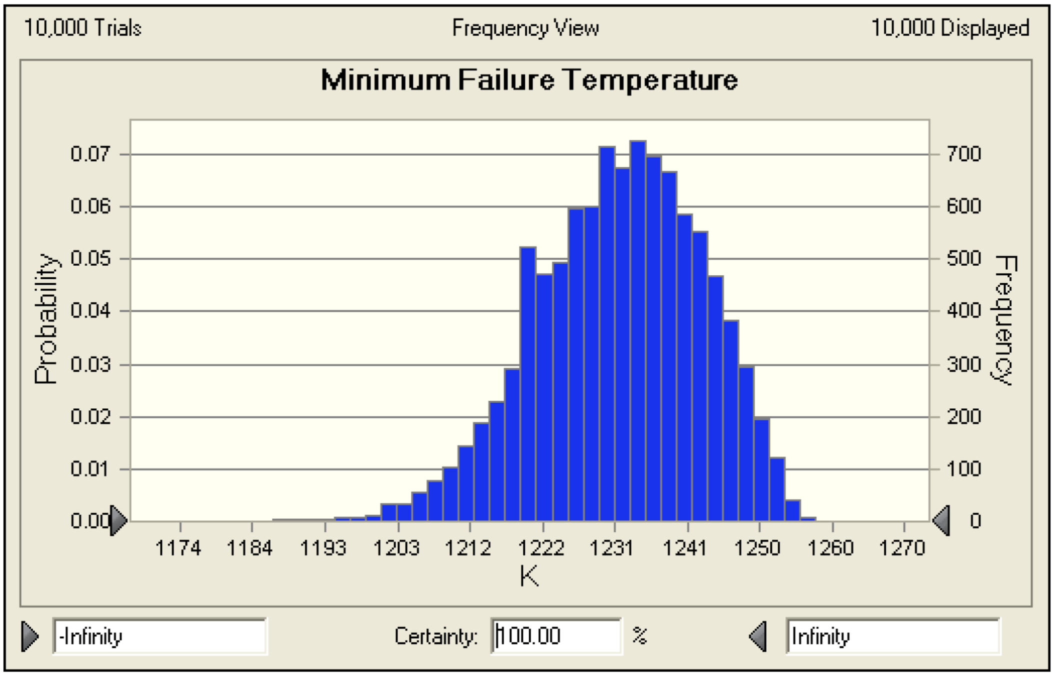

Source: Original

Figure D2.1-5. Probability Distribution for the Failure Temperature of Thick-Walled Canisters

D2.1.5.2 Probabilistic Analysis to Determine the Maximum Canister Temperature and Canister Failure Probability

The next step in the fragility analysis was to determine the maximum temperature of the canister as a result of the fire. In this analysis, Monte Carlo techniques were used to repeatedly sample from the uncertainty distributions discussed in Section D2.1.4 while applying the canister heating models to determine the maximum temperature of the canister due to the fire. As with the failure temperature analysis, Crystal Ball was used to perform the Monte Carlo simulation.

For each Monte Carlo sample, the calculated maximum canister temperature was then compared to a canister failure temperature sampled from the probability distribution discussed in Section D2.1.5.1. The canister is considered failed if the maximum temperature of the canister exceeded the sampled failure temperature for that Monte Carlo sample. The failure probability was determined as the fraction of the samples for which failure was calculated.

This process was repeated for a sufficient number of samples to provide a good statistical basis for the failure probability. The rule of thumb used in determining the required number of samples was that at least 10 failures had to be calculated. Thus, if the failure probability was on the order of 10^{-4}, 100,000 (10^{5}) samples were needed. The maximum number of samples for any run was set at 1 million. If no failures were calculated for one million samples, the failure probability was recorded as being less than 10^{-6}.

Since each Monte Carlo sample has two possible outcomes (failure or no failure), each sample represents a Bernoulli trial. Since the probability of failure or no failure is the same for each trial, the outcome from the sampling process can be represented by a binomial distribution. The binomial distribution is closely approximated by a normal distribution if the number of failures is greater than about five. The mean of the normal distribution is simply the number of failures divided by the total number of samples. The standard deviation of the normal distribution is given by the following Equation D-24:

$$\sigma = \sqrt{\frac{\frac{n_{fail}}{N}\left(\frac{N - n_{fail}}{N}\right)}{N}} \qquad \text{(Eq. D-24)}$$

where n_{fail} is the number of failures, N is the total number of Monte Carlo samples, and p_{fail} is the calculated mean failure probability (n_{fail}/N).

Figure D2.1-6 shows the calculated distribution for the maximum temperature reached by a thin-walled canister inside a waste package. The figure shows that the vast majority of the Monte Carlo samples had maximum temperatures well below 950°K. Only under extreme combinations of fire temperature and duration did the calculated maximum temperature approach the failure temperatures shown in Figure D2.1-4. Consequently there were only 32 calculated canister failures out of a total of 100,000 Monte Carlo samples. The resulting mean value for the canister failure probability is therefore 32/100,000 or 3.2×10^{-4}. The standard deviation calculated using Equation D-24 is 5.7×10^{-5}. The mean and standard deviation of the failure probability are shown in Table D2.1-8.

A similar analysis was performed for a thick-walled canister inside a waste package. Because of the thicker wall, the failure temperature of the canister is higher than for the thin-walled canister. In addition, the thick-walled canister heats up more slowly than the thin-walled canister because of its greater mass. These two factors combine to substantially lower the probability of failure for these canisters. In the Monte Carlo analysis, 20 failures were calculated for 200,000 samples, which results in a mean failure probability of 1×10^{-4} and a standard deviation of 2.2×10^{-5}.

Similar calculations have been performed for a canister inside a transportation cask and a canister inside the shielded bell of the CTM. The resulting mean and standard deviation for the canister failure probability are provided in Table D2.1-8.

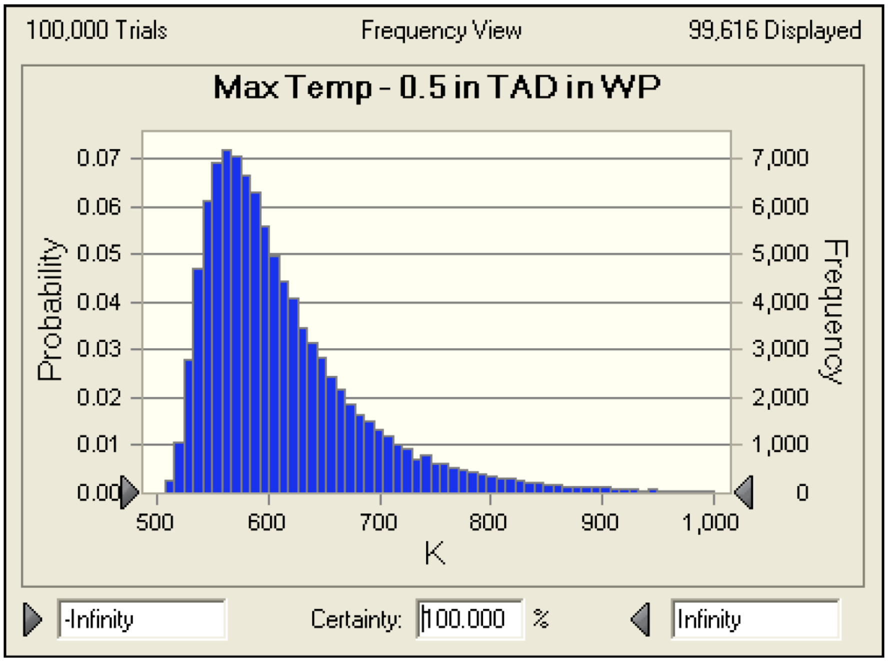

NOTE: TAD = transportation, aging, and disposal (canister); WP = waste package.

Source: Original

Figure D2.1-6. Probability Distribution for Maximum Canister Temperature – Thin-Walled Canister in a Waste Package

Table D2.1-8. Summary of Canister Failure Probabilities in Fire

Configuration[b]	Monte Carlo Results: Total Failures	Monte Carlo Results: Total Trials	Failure Probability: Mean	Failure Probability: Standard Deviation
Thin-Walled Canister in a Waste Package[a]	32	100,000	3.2×10^{-4}	5.7×10^{-5}
Thick-Walled Canister in a Waste Package[a]	20	200,000	1.0×10^{-4}	2.2×10^{-5}
Thin-Walled Canister in a Transport Cask	2	1,000,000	2.0×10^{-6}	1.4×10^{-6}
Thick-Walled Canister in a Transport Cask	1	1,000,000	1.0×10^{-6}	1.0×10^{-6}
Thin-Walled Canister in a Shielded Bell	27	200,000	1.4×10^{-4}	2.6×10^{-5}
Thick-Walled Canister in a Shielded Bell	27	300,000	9.0×10^{-5}	1.7×10^{-5}

NOTE: [a] For the 5-DHLW/DOE SNF waste package, this probability applies only to the DOE HLW canisters located on the periphery of the waste package. The DOE SNF canister in center of the waste package would not be heated appreciably by the fire.
[b] Configurations not addressed in this table include, any canister in a waste package that is inside the transfer trolley or any canister inside an aging overpack. In these configurations, the canister is protected from the fire by the massive steel transfer trolley or by the massive concrete overpack. Calculations have shown that the temperatures experienced by the canister in these configurations are well below the canister failure temperature. Although failures for these configurations could be screened on this basis, a conservative screening probability of 1×10^{-6} is used in the PCSA.

Source: Original

Note that Table D2.1-8 contains no failure probability for a bare canister configuration. The reason for this is that the canister is outside of a waste package or cask for only a short time.

During that time, the canister is usually inside the shielded bell of the CTM. The preceding analysis addressed a fire outside the shielded bell. When in that configuration, the canister is shielded from the direct effects of the fire. A fire inside the shielded bell, which could directly heat the canister, was not considered to be physically realizable for two reasons. First, the hydraulic fluid used in the CTM equipment is non-flammable (Ref. D4.1.48, p 30) and no other combustible material could be present inside the bell to cause a fire. Second, the annular gap between the canister and the bell only three inches wide, but is approximately 27 feet long. Given this configuration, it is unlikely that there would be sufficient inflow of air to sustain a large fire. There may be sufficient inflow to sustain a localized fire, but such a fire would not be adequate to heat the canister to failure.

The canister is also outside of a cask, waste package, or shielded bell as it is being moved from a cask into the shielded bell or from the shielded bell into a waste package. The time during which the canister would be in this configuration is extremely short (a matter of minutes) so a fire that occurs during this time is extremely unlikely. In addition, because the gap between the top of the waste package or cask and ceiling of the transfer cell is generally much shorter than the height of the canister, only a small portion of the canister surface would be exposed to the fire. Furthermore, this exposure would only be for the short time that the canister was in motion.

For these reasons, failure of a bare canister was not considered a physically realizable threat to breach of a canister and was not treated further.

The notes to Table D2.1-8 mention two other configurations for which fire-induced canister failure is not credible: a fire outside a waste package inside a waste package transfer trolley (WPTT) and a fire outside an aging overpack. These two special cases are discussed below.

The failure probability for a waste package in the WPTT was determined using the probabilistic methodology discussed above. For this calculation, the waste package calculation discussed earlier was modified by simply adding a thermal barrier outside the waste package to represent the WPTT. The fire heats the WPTT which then transfers heat by radiation to the outer barrier of the waste package. The WPTT was modeled as having an equivalent external diameter of 3.05 m, a thickness of 20.3 cm (steel thickness only[1]), and a mass of 89,000 kg. The transfer trolley was considered to be made of a stainless steel with an average specific heat of 476 J/kg K. The probabilistic analysis was run for 1 million Monte Carlo samples and no failures were calculated. Though the maximum temperature calculated in this analysis was well below the failure temperatures shown in Figures D2.1-4 and D2.1-5, a conservative failure probability of 1×10^{-6} is used in the PCSA.

The probabilistic methodology discussed above could not be used for analysis of canister failure for a fire outside an aging overpack. The reason for this is that the concrete that comprises the majority of the aging overpack has a very low thermal conductivity. Therefore, the underlying premise of a relatively uniform temperature in each cylindrical region would be incorrect. Instead, a simple heat conduction calculation was performed to determine how far into the concrete heat could be conducted during a fire. The thermal penetration depth (from

[1] There is also a 7.5-inch layer of borated polyethylene. Because this layer is likely to melt early in the fire transient, it is ignored in the analysis.

Equation D-11) was estimated based on a bounding 2-hour fire and concrete with the following average properties: thermal conductivity = 1.2 W/m K; density = 2,200 kg/m^3; and specific heat = 1,000 J/kg K. The thermal penetration depth calculated for these conditions was 6.3 cm. Since the aging overpack is expected to be at least 24 inches (61 cm) thick, the canister inside the aging overpack will not be heated significantly by the fire. A conservative failure probability of 1×10^{-6} is used in the PCSA.

Note that, in this calculation, the fire was modeled as being only on the outside of the aging overpack. Though the overpack has ventilation openings for natural circulation, this flow path is expected to provide sufficient resistance to airflow that (1) combustion could not be sustained inside the overpack even if fuel entered through the openings, and (2) hot gases would likely flow over the outer surface of the overpack rather than enter the ventilation openings and flow up through the annulus inside the overpack. In fact, because oxygen would be consumed by the fire near the bottom of the overpack, air may actually flow downward through the ventilation openings to supply air to the fire.

D2.1.5.3 Analysis To Determine Failure Probabilities For Bare Fuel in Casks Exposed To Fire

Another fire-induced failure mode is of interest in the PCSA; namely, failure of a transport cask containing bare spent fuel assemblies. The analysis uses GA-4/GA-9 transportation casks to represent casks of this type. Should a transportation cask containing uncanistered spent nuclear fuel fail in a fire, it is of interest for determining the source term to know if the fuel cladding is heated above its failure temperature (approximately 700°C to 800°C).

A modified version of the model for failure of a canister in a transportation cask was used to determine the probability that fuel will exceed this failure temperature. In the modified spreadsheet, the canister was replaced by the mass of fuel that would be heated during the fire. As in the bare canister analysis discussed in Section D2.1.4.1, this mass was estimated based on the calculated thermal penetration depth. Based on the information provided in the GA-9 SAR report (Ref. D4.1.34, p. 3.6-3), the following average spent fuel properties were determined: thermal conductivity = 1.5 W/m K, density × specific heat = 9.9×10^5 J/m^3 K. For a 1-hour fire, the calculated thermal penetration depth is 7.4 cm and the effective fuel mass is 1,910 kg. Since the severe fires of greatest concern have durations of 1 hour or longer, this fuel mass represents a reasonable, but probably conservative, estimate.

Other modifications to the model included changes to model the geometry and materials used in the GA-4/GA-9 casks. The inputs to the model are presented in Table D2.1-9. As in the previous analyses, the model does not rely on neutron shield because it is liable to melt early in the transient.

The model was run for three different fuel failure temperatures: 700°C, 750°C, and 800°C. This range of failure temperatures represents the lower end of the values reported in the literature (Ref. D4.1.65, pp. 7-20 to 7-21). As shown in Table D2.1-10, the calculated fuel failure probabilities were less than 0.001.

Table D2.1-9. Model Inputs – Bare Fuel Cask

Model Parameter	Value	Basis/Rationale
Fuel Properties		
Heated Mass (kg)	1,910	Calculated based on thermal penetration depth (see text)
Specific Heat (J/kg K)	438	Average for fuel region taken from *Thermal Responses of TAD and 5-DHLW/DOE SNL Waste Packages to a Hypothetical Fire Accident* (Ref. D4.1.25, Table 15)
Effective Surface Area (m^2)	10.0	Projected area for radiation heat transfer. Calculated based on equivalent outer diameter of fuel region (0.66 m)
Emissivity	0.8	From *Thermal Responses of TAD and 5-DHLW/DOE SNL Waste Packages to a Hypothetical Fire Accident* (Ref. D4.1.25, Table 17)
Initial Temperature (K)	400	Estimated from fig 3.4-4 in GA-9 SAR (Ref. D4.1.34)
Transportation Cask Outer Shell		
Outer Diameter (m)	1.12	Equivalent diameter estimated based on GA-9 SAR (Ref. D4.1.34, Figure 1.2-9)
Wall Thickness (m)	0.0032	Minimum outer shell thickness listed in cask SAR (Ref. D4.1.34)
Length (m)	4.25	Length adjacent to the fuel region
Density (kg/m^3)	7850	Density of 516 carbon steel (Ref. D4.1.6, Section II, Part A, SA-20, 14.1)
Specific Heat (J/kg K)	604	Approximate value for 516 carbon steel at 400°C (Ref. D4.1.25, Table 10)
Emissivity	0.8	Average value for carbon steel in Avallone and Baumeister, (Ref. D4.1.8, Table 4.3.2)
Initial Temperature (K)	344	Estimated from fig 3.4-4 in GA-9 SAR (Ref. D4.1.34)
Transportation Cask Gamma Shield[a]		
Outer Diameter (m)	0.902	Equivalent diameter estimated based on GA-9 SAR (Ref. D4.1.34, Figure 1.2-9)
Wall Thickness (m)	0.107	Combined thickness of stainless steel and depleted uranium shields (steel: 0.0445 m; DU: 0.0622 m)(Ref. D4.1.34)
Length (m)	4.25	Length adjacent to the fuel region
Mass × Specific Heat (J/K)	3.45×10^6	Based on calculated masses of steel and DU and specific heats listed in GA-9 SAR (Ref. D4.1.34, Tables 2.2-1 and 3.2-2)
Emissivity	0.8	Average value for carbon steel in Avallone and Baumeister, (Ref. D4.1.8, Table 4.3.2)
Initial Temperature (K)	360	Estimated from fig 3.4-4 in GA-9 SAR (Ref. D4.1.34)
Post-Fire Conditions		
Ambient Temperature (K)	361	Post-fire temperature of 190°F from *Discipline Design Guide and Standards for Surface Facilities HVAC Systems* Ref. D4.1.16, Section 3.2). This value is 100 °F higher than the maximum interior facility temperature

Table D2.1-9. Model Inputs – Bare Fuel Cask (Continued)

Model Parameter	Value	Basis/Rationale
Heat Transfer Coefficient (W/m^2 K)	2.0	Natural convection based on anticipated post-fire surface temperature and standard convective heat transfer correlations (Results not sensitive to this value)

NOTE: [a] Composite properties representing both the stainless steel cask wall and depleted uranium gamma shield.
DU = depleted uranium

Source: Original

Table D2.1-10. Summary of Fuel Failure Probabilities

Fuel Failure Temperature	Monte Carlo Results		Failure Probability	
	Total Failures	Total Trials	Mean	Standard Deviation
700°C	54	100,000	5.4×10^{-4}	7.4×10^{-5}
750°C	27	100,000	2.7×10^{-4}	5.2×10^{-5}
800°C	13	100,000	1.3×10^{-4}	3.6×10^{-6}

Source: Original

D2.1.5.4 Analysis To Determine Failure Probabilities For Casks Exposed To Fire

NUREG/CR-6672 (Ref. D4.1.65, Section 6) provides an analysis of seal failure in bare fuel transportation casks. The analysis uses a simple 1-D axisymmetric heat transfer model that is similar to the simple model used in the fire fragility analysis presented in Section D2. The simple model is used to determine the length of time the cask could be exposed to an 800°C or 1,000°C fire before seal failure would be predicted.

The report notes that the elastomer seals used in many transportation casks degrade completely at 500°C, but that the degradation rate increases significantly at 350°C (Ref. D4.1.65, p. 2-9). Other seal degradation information provided by cask vendors indicates that the maximum design temperature for the metallic o-ring seals in the TN-68 casks is 536°F (280°C) (Ref. D4.1.66, p. 3-2). This is the maximum safe temperature for continuous operation. The actual failure temperature for these seals would be much higher. Based on this information, seal failure is anticipated at temperatures of around 350°C to 450°C.

NUREG/CR-6672 indicates that the seals in a steel/depleted uranium truck cask would reach 350°C if exposed to a 1,000°C fire for 0.59 hours (Ref. D4.1.65, Table 6.5). In a steel-lead-steel (SLS) truck cask, this temperature would be reached in 1.04 hours. The times for rail casks were longer at 1.06 hours for an SLS rail cask and 1.37 hours for a monolithic steel rail cask.

The probability distributions for fire temperature and fire duration discussed in section D2.1.1 can be used to determine the probability that the fire conditions listed in the preceding paragraph would be exceeded. This is accomplished by first determining the probability distribution (using Crystal Ball) for the maximum thermal radiation energy from the fire using the following Equation D-25:

$$Q_{rad} = \sigma A T_{fire}^4 t_{fire} \qquad \text{(Eq. D-25)}$$

where

σ	=	the Stefan-Boltzmann constant (5.668×10^{-8} W/m^2 K^4)
A	=	cask surface area exposed to the fire
T_{fire}	=	fire temperature (sampled from the probability distribution)
t_{fire}	=	fire duration (sampled from the probability distribution)

The probability distribution for Q_{rad} is shown in Figure D2.1-7:

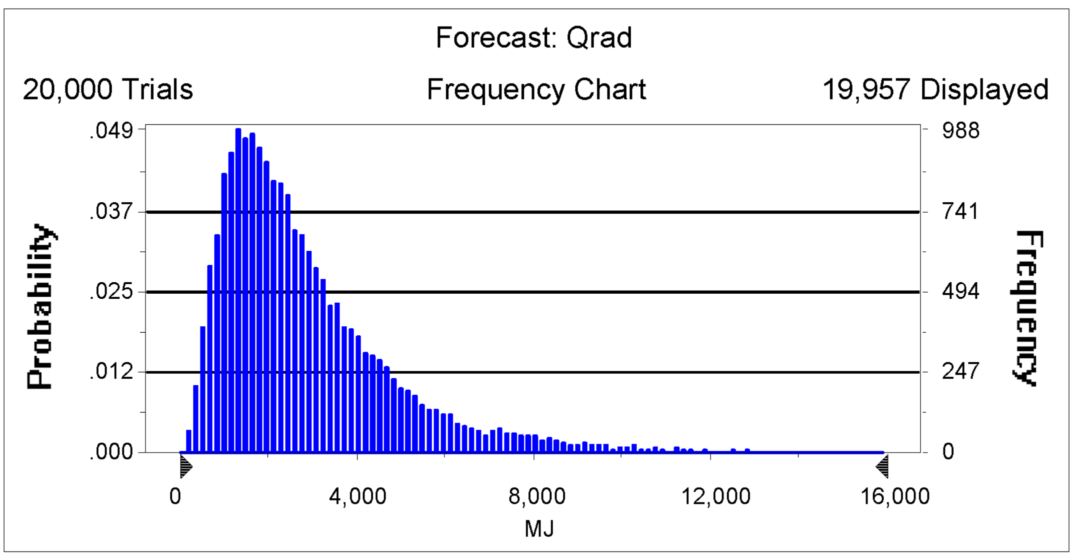

Source: Original

Figure D2.1-7. Distribution of Radiation Energy from Fire

Next, the value for Q_{rad} corresponding to the NUREG/CR-6672 (Ref. D4.1.65) fire temperature and duration for seal failure is calculated. The probability distribution for Q_{rad} can then be used to determine the probability that the fire will be severe enough to cause seal failure (i.e., will exceed the value for Q_{rad} calculated based on the NUREG/CR-6672 conditions).

The values for Q_{rad} corresponding to a 1,000°C fire and the fire durations reported in NUREG/CR-6672 (Ref. D4.1.65) are listed below along with the probability of exceedance determined from the probability distribution. The exceedance probabilities can be used as an estimate of the seal failure probability for seals that fail at the temperature, T_{fail}, listed in Table

D2.1-11. For example, for a SLS truck cask that has seals that fail at 350°C, the probability that the seals fail due to a fire is 6.9×10^{-3}.

By multiplying the highest seal failure probability in Table D2.1-11 (0.05) by the highest probability of fire-induced cladding failure in Table D2.1-11 (5.4×10^{-4}), it is shown that the joint conditional probability of a fire that causes additional cladding failure in a truck cask, given a fire, is less than 3×10^{-5}. Because the fire initiating event frequency over the preclosure period of such truck cask fires is less than 1 (see Attachment F for the facilities that contain these, i.e., WHF and Intra-Site operations), such fires are beyond Category 2 and not analyzed further.

Table D2.1-11. Probabilities that Radiation Input Exceeds Failure Energy for Cask

Cask Type	T_{fail} (°C)	Temperature (°C)	Duration (hrs)	Q_{rad} (MJ)	P_{exceed}
Steel/DU Truck Cask	350	1,000	0.59	7,208	5.0×10^{-2}
Steel/Lead/Steel Truck Cask	350	1,000	1.04	12,405	6.9×10^{-3}
Steel/Lead/Steel Rail Cask	350	1,000	1.06	12,950	5.6×10^{-3}
Monolithic Steel Rail Cask	350	1,000	1.37	16,737	1.7×10^{-3}
Steel/DU Truck Cask	500	1,000	≈ 1.0[a]	≈ 12,200	7.1×10^{-3}
Steel/Lead/Steel Truck Cask	500	1,000	≈ 1.3[a]	≈ 15,900	2.2×10^{-3}

NOTE: [a] Estimated from Figure 6.6 in NUREG/CR-6672 (Ref. D4.1.65).
DU = depleted uranium; hrs = hours; MJ = megajoules.

Source: Original

D2.2 SHIELDING DEGRADATION IN A FIRE

The NUREG/CR-6672 (Ref. D4.1.65) transportation study performed analyses on the internal temperatures of cask for long duration fires of 1,000°C. The transportation study included scenarios for fire-only and fire-plus-impact in the calculation of the probability of loss of shielding (LOS).

D2.2.1 Analysis of Loss of Shielding for Transportation Casks

All transportation casks contain separate gamma and neutron shields. The neutron shields are generally composed of a low melting point polymer material that would melt and offgas very quickly when exposed to a fire. For that reason, it is given that the neutron shield is always lost in fire scenarios. The composition of the gamma shield varies between cask designs, with some designs having layers of steel and depleted uranium, others having layers of steel and lead, or and others with layers of steel. Only casks containing lead could lose their gamma shielding in a fire.

As previously discussed, the thermal analyses for the transportation casks (Ref. D4.1.65, Table 6.5) shows that the internal regions of the cask reach the 350°C range in the range of 0.59 to 1.37 hours for the long duration 1,000°C fire. The least time represents the steel- depleted uranium casks and the longest the monolithic steel. The time to reach 350°C for SLS casks is about one hour. The time to reach the lead melting temperature (327.5°C) should be somewhat less than one hour but is not specified. However, NUREG/CR-6672 (Ref. D4.1.65) indicates that lead melting in itself does not result in significant LOS but the melting must be accompanied by outer shell puncture that permits the lead to flow out of the shield configuration.

NUREG/CR-6672 states that there are four characteristic fires of interest in the transportation risk analysis: 10 minutes as the duration of a typical automobile fire; 30 minutes for a regulatory fires; 60 minutes for an experimental pool fire for fuel from one tanker truck; and 400 minutes for an experimental pool fire from one rail tank car. These typical durations suggest that a real fire is unlikely to last long enough to result in a LOS condition for transportation scenarios.

D2.2.2 Probability of LOS in Fire Scenarios

Melting of the lead shielding and loss of containment of the molten lead results in loss of shielding for SLS casks. Two mechanisms for escape of the molten lead are considered:

- Puncture of the outer shell
- Rupture lead containment due to internal pressure

Puncture of the 2-inch thick (or more) outer shell, in addition to exposure to fire, would allow molten lead to escape, resulting in LOS. The shell puncture would be an independent failure with a probability of 10^{-8} for the low speeds at which the cask would be moving (Table 6.3-4). With the additional failure of exposure to fire, the LOS probability would be even less.

Containment of the molten lead could be lost due to thermal expansion of the lead coincident with the thermal weakening of the steel. Molten lead is cast into the cavity bounded by the inner and outer shells and the bottom plate ((Ref. D4.1.50, p. 1.1-4); (Ref. D4.1.49, p. 1.2-2); (Ref. D4.1.9, p. 1.2-5); and (Ref. D4.1.47, p. 1-5)). The lead contracts as it cools and solidifies. When the cask is exposed to a fire and the lead melts, it expands to reoccupy the volume when originally cast. When heated beyond the melting point, the liquid lead could continue to expend, exerting hoop stresses upon the inner and outer shells. The shells are thick and strong, e.g. the inner and outer shell thicknesses for the MP197 are 1.25 and 2.5 inches, respectively (Ref. D4.1.47, Drawing 1093-71-4, rev. 1), and the bottom plate thickness is 6.5 inches (Ref. D4.1.47, Drawing 1093-71-2, rev. 1). Consequently, failure of the steel is considered very unlikely.

As part of the PCSA, an attempt was made to analyze hydraulic failure of the molten lead containment due to a fire. Unfortunately, the thermal and physical properties of lead necessary for this analysis could not be found. Thus, hydraulic failure cannot be conclusively disproved. For that reason, a probability of 1.0 is used for LOS by transportation casks due to fire.

D2.2.3 Bases for Screening of Loss of Shielding Pivotal Events for Aging Overpacks in Fire Scenarios

This section summarizes the rationale for screening loss of shielding pivotal events associated with heating of aging overpacks in a fire. Loss of shielding could occur if the concrete that comprises the majority of the aging overpack spalled as a result of the fire. Spalling would reduce the thickness of the concrete and, if sufficient spalling occurs, the thickness could be reduced below the level required for adequate shielding.

D2.2.3.1 Thickness of Concrete Required for Adequate Shielding

The concrete thickness needed for adequate shielding can be estimated by determining the dose outside the overpack for different concrete thicknesses and comparing that dose to the exposure limits for radiation workers. For this calculation, the exposure rate on the surface of the aging overpack prior to the fire is 40 mrem/hr (Ref. D4.1.15, Section 33.2.4.17).

The dose outside the aging overpack is primarily due to Co-60 gamma radiation, the gamma attenuation due to concrete can be estimated based on data available from the National Institute of Standards and Technology (NIST) (Ref. D4.1.40). This reference lists a value for the mass attenuation coefficient of the concrete divided by the concrete density (μ/ρ) of 0.058 cm^2/g for the gammas produced by Co-60. Multiplying this value by an approximate concrete density of 2.3 g/cm^3 (Ref. D4.1.39, Table 4.2.5) yields a value for the mass attenuation coefficient of 0.133 cm^{-1}. Based on this value, there is approximately a factor of 10 reduction in the gamma dose for each 17.2 cm (6.8 inches) of concrete.

If the outer 6.8 inches of concrete were to spall as a result of the fire, the dose at the surface of the aging overpack would increase to 400 mrem/hr. If an additional 6.8 inches of concrete were to spall, the dose on the surface would be 4 rem/hr. The original concrete thickness is 34 inches based on existing aging overpack drawings (Ref. D4.1.14). There is 27.2 inches of concrete remaining after the first 6.8 inches of spallation and 20.4 inches of concrete remaining after the second 6.8 inches of spallation.

The dose outside the aging overpack can be estimated by noting that the dose decreases as the square of the distance from the source. After 13.6 inches of concrete has spalled, the dose 20.4 inches from the surface of the aging overpack would be 1 rem/hr, and the dose 61.2 inches from the surface would be 250 mrem/hr. Therefore, even in the case of extensive concrete spalling, workers involved in fire fighting or post-fire activities could be in close proximity to the degraded aging overpack for a lengthy period of time without exceeding either the annual exposure limit of 5 rem or special exposure limits outlined in 10 CFR Part 20 (Ref. D4.2.1, Paragraph 20.1206).

D2.2.3.2 Extent of Concrete Spalling in a Fire

The current aging overpack design has a steel liner outside the concrete shielding. Consequently, spalling and removal of concrete from the surface cannot occur unless the steel liner is removed or fails catastrophically. However, because alternative aging overpack designs have been considered without a steel outer liner, the potential for substantial spallation with a bare concrete shield was assessed.

Extensive spalling of structural concrete has been observed under some conditions when the structural concrete is exposed to intense fires. The most extensive spalling has been observed in tunnel fires, such as the Channel Tunnel fire in 1996. In such cases, a significant fraction of the concrete spalled when exposed to the intense heat from the long-duration fires.

Due to the potential significance of spalling in reducing the strength of concrete support structures, spallation of concrete has been the subject of considerable study. "Limits of Spalling of Fire-Exposed Concrete." (Ref. D4.1.37) provides a good overview of the factors that control concrete spalling due to fire. Hertz indicates that that there are three types of spalling that can occur: (1) aggregate spalling, (2) explosive spalling, and (3) corner spalling. Aggregate spalling occurs with some aggregates (such as flint or sandstone) and results in superficial craters on the surface of the concrete. Corner spalling occurs only on the convex corners of beams or other structures and is caused by a localized weakening and cracking of the concrete such that the corner breaks off under its own weight. This mode of spalling is not relevant for the aging overpacks. Explosive spalling occurs when sufficient pressure builds up inside the concrete to cause pieces of concrete to be ejected from the surface. Explosive spalling is believed to account for the extensive concrete loss observed in the Channel Tunnel fire. Of the three modes of spalling, only explosive spalling could produce the loss of concrete necessary to significantly reduce the shielding capability of the aging overpack.

"Predicting the fire resistance behaviour of high strength concrete columns," (Ref. D4.1.43) notes that explosive spalling occurs when sufficient pressure builds up in the pores of the concrete to cause ejection of concrete from the surface. Buildup of such a high pressure requires three things: (1) low concrete permeability, (2) high moisture content in the concrete, and (3) rapid heating and resulting large thermal gradients. In addition, "Limits of Spalling of Fire-Exposed Concrete." (Ref. D4.1.37) notes that spallation is more pronounced in concrete structures undergoing high compressive stress, such as support columns.

Low permeability prevents gas migration and allows pressure to build. High structural strength concretes, such as those used in tunnel construction, are known to have very low permeability and are therefore more prone to spalling. In contrast, normal strength concretes do not have low permeability and spallation is not observed (Ref. D4.1.43). Because the concrete used for shielding in the aging overpacks is not counted on for structural strength and is therefore classified as normal strength concrete[2], spallation is unlikely to occur.

Moisture content is a major factor in pressure buildup because water vapor is the gas primarily responsible for high pore pressures in the concrete. The concrete in the aging overpacks is unlikely to have a high moisture content because it is heated both internally by decay heat and externally by solar heat. In addition, it is likely to have been sitting in the Nevada desert for a lengthy period of time.

Thus, although the fire will produce large thermal gradients in the concrete, these gradients are unlikely to result in pressure buildup sufficient to cause extensive spallation due to the expected high permeability and low moisture content of the aging overpack concrete. This would be true regardless of whether the outer steel liner is present or not.

D2.2.3.3 Conclusion

The preceding discussion has shown that a substantial amount of concrete would have to spall during a fire to produce a hazard to workers involved in either fire fighting or post-fire activities. In addition, it was shown that spallation is very unlikely given the type of concrete to be used in

[2] For example, the compressive strength of the concrete used in the HI-STORM storage overpack (Ref. D4.1.39, Table 1.D.1) is listed as 3,300 psi or 22.75 MPa, which is well below the strength of 55 MPa usually defined as necessary for high strength concrete (Ref. D4.1.43).

the aging overpacks and the likelihood that the aging overpacks will have an outer steel liner. For these reasons, loss of aging overpack shielding in a fire is considered Beyond Category 2 and need not be analyzed further.

D3 SHIELDING DEGRADATION DUE TO IMPACTS

Neutrons emitted from transportation casks are shielded by a resin surrounded by a steel layer. The neutron shielding is present in the top lid, bottom and shell. Neutron shields designed to 10 CFR Part 71 (Ref. D4.2.2) are robust against 10 CFR Part 71 hypothetical accident conditions related to impacts or drops, exhibiting factors of safety greater than 1 for Service Level D allowables. Meeting *2004 ASME Boiler and Pressure Vessel Code* Service Level D (Subsection NF) (Ref. D4.1.6) provides for twice the allowable stress intensity as normal operation but still results in an extremely low failure probability. In addition, neutron dose typically attenuates quickly with distance from the transportation cask so it is only a small fraction of the gamma dose to personnel more than two meters away. Evacuation to that distance is the way to reduce personnel dose from neutrons. For these reasons, the analysis below focuses on the principle threat to workers on the site, which is degradation of gamma shielding.

This section summarizes information on loss of shielding mechanisms that could occur in event sequences for repository waste handling operations. The information is derived from transportation cask accident risk analyses. This information provides insights and bases for estimating probabilities of passive failures that result in LOS for casks and overpacks in waste handling event sequences.

The repository facilities process three categories of waste containers that provide shielding: transportation casks (truck and rail) and aging overpacks. The event sequence diagrams for operations involving processing of transportation casks and aging overpacks include the pivotal event "loss of shielding" for event sequences that are initiated by physical impact or fire. LOS due to fire was addressed previously in section D2.2 of this attachment. The following discussion focuses specifically on LOS due to drops and impacts.

The information in this section is based in large part on results of FEA performed for four generic transportation cask types for transportation accidents as reported in NUREG/CR-6672 (Ref. D4.1.65) and NUREG/CR-4829 (Ref. D4.1.32). The results of the FEA were used to estimate threshold drop heights and thermal conditions at which LOS may occur in repository event sequences, using damage severity levels keyed to the FEA results to determine the challenge needed to cause LOS. The four cask types included one steel monolith rail cask, one steel/depleted uranium truck cask, one SLS truck cask and one SLS rail cask. NUREG/CR-6672 states that the steel in any of the cask is thick enough to provide some shielding, but the depleted uranium and lead provide the primary gamma shielding for the multi-shell cask types. The referenced study performed structural and thermal analyses for both failure of containment boundaries and loss of shielding for accident scenarios involving rail cask and truck cask impacting unyielding targets at impact speeds of 30-60, 60-90, 90-120, and greater than120 mph. The impact orientations included side (0–20 degrees), corner (20 degrees–85 degrees), and end (85 degrees–90 degrees). The referenced study also correlated the damage from impacts on real targets including soil and concrete.

The event sequences used in the transportation accident analyses included impact-only, impact plus-fire, and fire-only conditions. The results of the FEA indicate that LOS could occur in the impact-only at speeds as low as 30 mph with an unyielding target and in fire scenarios of sufficient intensity and duration. The structural analyses did not credit the energy absorption capability of impact limiters. Therefore, the results are deemed applicable to approximate the structural response of transportation and similar casks in drop scenarios.

The primary reference NUREG/CR-6672 (Ref. D4.1.65), however, does not provide a threshold below which no LOS could be assured. Therefore, information quoted in an evaluation by the Association of American Railroads (Ref. D4.1.30) was used to establish thresholds for LOS conditions based on damage categories that are correlated to plastic strain in the inner shell of a cask. That information is based on a prior transportation accident analysis known as the Modal Study (Ref. D4.1.32). For potential PCSA applications, FEA results for inner shell strain versus impact speed were extended to estimate the lower bound of impact speed or drop heights to establish conditions at which LOS may occur in cask-drop scenarios in repository operations.

NUREG/CR-6672 (Ref. D4.1.65) addresses two modes of LOS in accident scenarios: deformations of lid and closure geometry that permit direct streaming of radiation; and/or reductions in cask wall thickness or relocation of the depleted uranium or lead shielding. The LOS due to lid/closure distortion can be accompanied by air-borne releases if the inner shell of the cask is also breached.

The results of the FEA reported in NUREG/CR-6672 (Ref. D4.1.65) provides some definitive results that are deemed to be directly applicable to the repository event sequence analyses:

- Monolithic steel rail casks do not exhibit any LOS, but there may be some radiation streaming through gaps in closure in any of the impact scenarios. This result can be applied to both transportation casks.

- Steel/depleted uranium/steel truck cask exhibited no LOS, explained by modeling that included no gaps between forged depleted uranium segments so that no displacement of depleted uranium could occur.

- The SLS rail and truck casks exhibit LOS due to lead slumping. Lead slump occurs mostly on end-on impact with a lesser amount in corner orientation. For side-on orientation, there is no significant reduction in shielding.

Therefore, this analysis focuses on LOS for SLS casks to estimate the drop or collision conditions that could result in LOS from lead slumping. Figure D3.2-1 illustrates the effect of cask deformation and lead slumping for a SLS rail cask following an end-on impact at 120 mph onto an unyielding target from the result of the FEA reported in NUREG/CR-6672 (Ref. D4.1.65).

D3.1 DAMAGE THRESHOLDS FOR LOS

The Association of American Railroads study (Ref. D4.1.30) is used as a reference for this report. The information cited, however, was derived from an earlier transportation cask study known as the "Modal Study," (Ref. D4.1.32). The Modal Study assigned three levels of cask response characterized by the maximum effective plastic strain within the inner shell of a transport cask. The severity levels are defined as:

- S1–implies strain levels < 0.2%
- S2–implies strains between 0.2 and 2.0%
- S3–implies strain levels between 2.0 and 30%.

The amount of damage to a cask for the respective severity levels is summarized in the following:

S1:

- No permanent dimensional change
- Seal and bolts remain functional
- Little if any radiation release
- Less than 40 g axial force on lead for all orientations
- No lead slump
- Fuel basket functional; up to 3% of fuel rods may release into cask cavity
- Loads/releases within regulatory criteria.

S2:

- Small permanent dimensional changes
- Closure and seal damage; may result in release
- Limited lead slump
- Up to 10% of fuel rods release to cask cavity.

S3:

- Large distortions
- Seal leakage likely
- Lead slump likely
- 100% fuel rods release to cask cavity.

As stated above, limited lead slumping may occur at damage level S2, but is likely to occur at damage level S3. The respective strain levels associated with damage levels S2 and S3 were applied to the results from NUREG/CR-6672 (Ref. D4.1.65) to establish a threshold impact speed for the onset of LOS.

D3.2 SEVERITY OF DAMAGE VERSUS IMPACT VELOCITY

The FEA results given in Table 5.3 of NUREG/CR-6672 (Ref. D4.1.65) are summarized in Table D3.2-1. The strain in the inner shell of the SLS casks are shown in Table D3.2-1 and illustrated in Figure D3.2-1. These data were plotted (Figures D3.2-2 and D3.2-3). The data points start at the lowest speed range of 30 to 60 mph. The data were plotted as points using the lower boundary of each of the four speed ranges on the abscissa. The strain plots were extended to the origin by including the point (0, 0) with the Table D3.2-1 data.

Two horizontal lines were superimposed on Figures D3.2-2 and D3.2-3 to plot the 0.2% and 2.0% strain to represent the respective S2 and S3 thresholds for inner shell strain. The intersections of the strain curves with the respective threshold values indicate the minimum impact speed at which the respective S2 and S3 strain thresholds appear to be exceeded.

Table D3.2-1. Maximum Plastic Strain in Inner Shell of Sandwich Wall Casks

Cask Type	Orientation: Speed, mph	Corner Impact Strain, %	End Impact Strain, %	Side Impact Strain, %
SLS Truck	30	12	3.9	N/A
	60	29	12	16
	90	33	18	24
	120	47	27	27
SDUS Truck	30	11	1.8	6
	60	27	4.8	13
	90	43	8.3	21
	120	55	13	30
SLS Rail	30	21	1.9	5.9
	60	34	5.5	11
	90	58	13	15
	120	70	28	N/A

NOTE: SDUS = steel-depleted uranium-steel; SLS = steel-lead-steel.

Source: From Ref. D4.1.65, Table 5.3

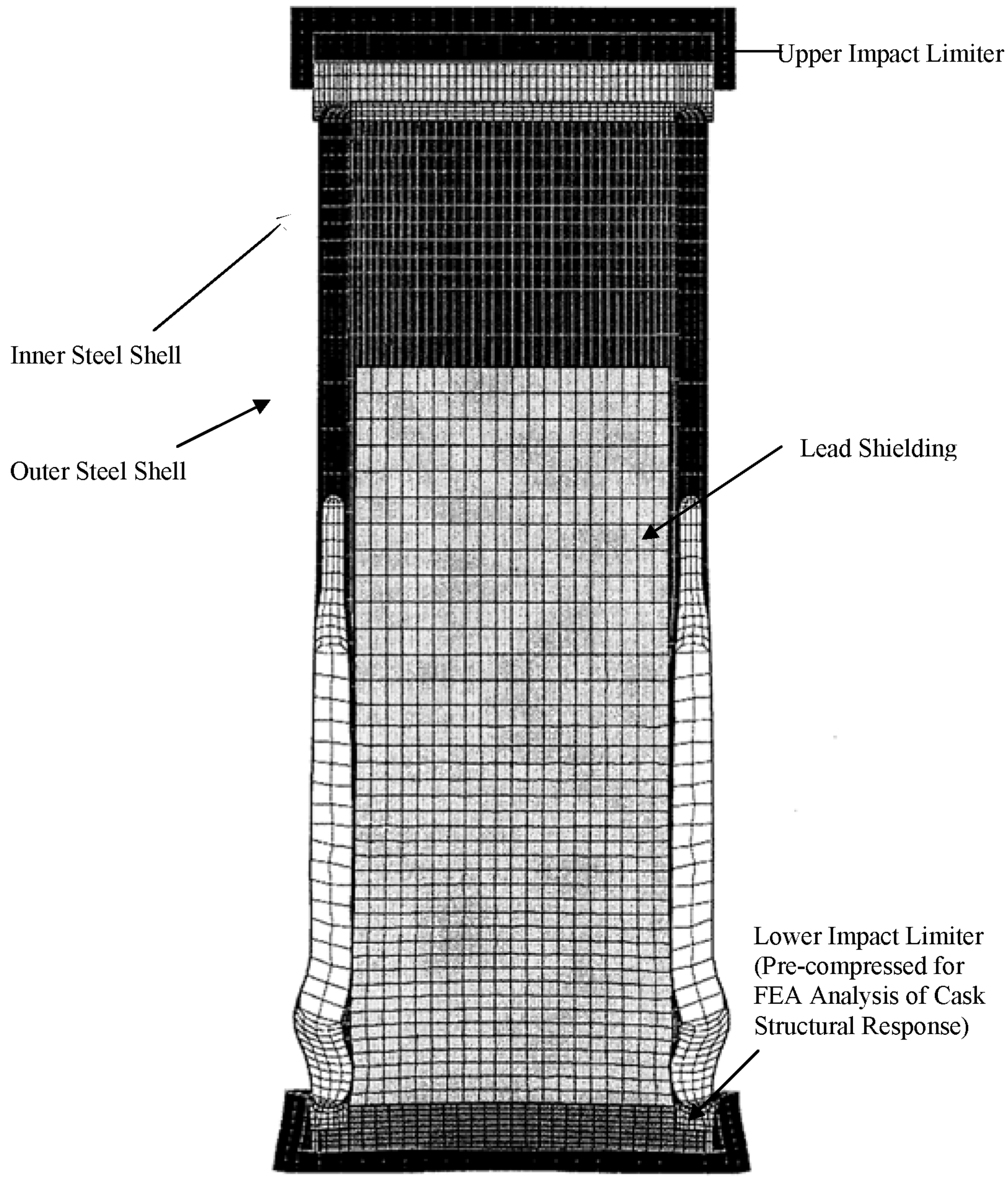

Source: From Ref. D4.1.65, Figure 5.9

Figure D3.2-1. Illustration of Deformation and Lead Slumping for a SLS Rail Cask Following End-on Impact at 120 mph

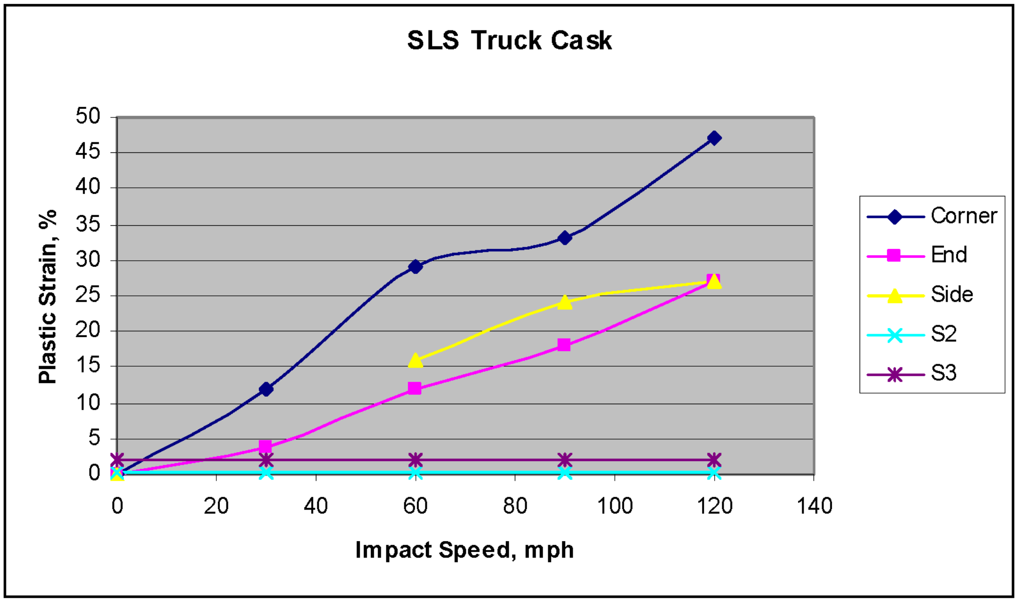

NOTE: [1] Data points for strain versus speeds greater than 30 mph taken directly from NUREG/CR-6672, Table 5.3: plots extended to origin (0,0) to determine crossover for S2 and S3 threshold strains.
[2] S2 and S3 threshold strains based on information in *A Railroad Industry Critique of the Model Study* (Ref. D4.1.30).

mph = miles per hour; SLS = steel-lead-steel.

Source: Original

Figure D3.2-2. Truck Steel/Lead/Steel Inner Shell Strain versus Impact Speed

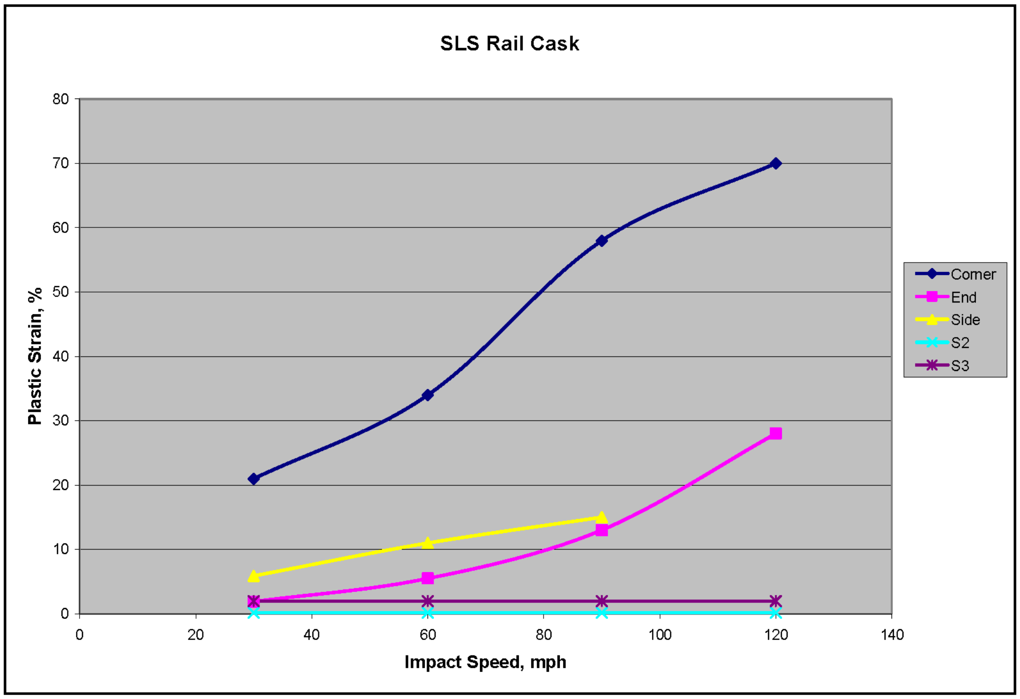

NOTE: [1] Data points for strain versus speeds greater than 30 mph taken directly from NUREG/CR-6672 (Ref. D4.1.65, Table 5.3): plots extended to origin (0,0) to determine crossover for S2 and S3 threshold strains.
[2] S2 and S3 threshold strains based on information in *A Railroad Industry Critique of the Model Study* (Ref. D4.1.30).

mph = miles per hour; SLS = steel-lead-steel.

Source: Original

Figure D3.2-3. Rail Steel/Lead/Steel Strain versus Impact Speed

D3.3 ESTIMATE OF THRESHOLD SPEEDS FOR LOSS OF SHIELDING DUE TO IMPACTS

The plots in Figures D3.2-2 and D3.2-3, and Table D3.2-1 illustrate that the S2 threshold is exceeded for both the truck and rail SLS casks for all four speed ranges and all orientations. Since NUREG/CR-6672 (Ref. D4.1.65) does not report LOS conditions for low impact speeds, it is concluded that the S2 criterion is not a valid threshold for LOS in SLS casks. Therefore, the remainder of this analysis applies the S3 criterion (2% shell strain) as a basis for estimating LOS threshold impact speeds.

Figures D3.2-2 and D3.2-3, and Table D3.2-1 indicate that the S3 threshold is exceeded for both truck and rail SLS casks for all orientations. The intersections of the strain curves and the 2% strain line in Figures D3.2-2 and D3.2-3 illustrate the impact speed at where the S3 threshold is reached for each case. A small exception being the end drop of a SLS rail cask in the 30-60 mph range for which the shell strain of 1.9% is just below the lower bound for S3 damage. However, this margin is too small to exclude that case. Although the strains for the side drop cases exceed the threshold for lead slumping, NUREG/CR-6672 (Ref. D4.1.65) states that lead slumping does not occur in side drops. Therefore, LOS for side drops is excluded from the remainder of this report.

Using the 2% shell strain condition as the threshold for LOS in SLS casks, the following is observed:

- LOS for the truck SLS cask would occur at impact speeds of about 5 mph for corner impact and about 18 mph for end impact
- LOS for the rail SLS cask would occur at about 3 mph for corner impact and about 30 mph for end impact.

It is observed that the corner drop cases give the largest shell strain at a given impact speed but the finite element analyses indicate that the extent of lead slumping is less in corner drops than for end impacts.

Table D3.3-1 shows the drop height equivalents for impact speed onto a horizontal unyielding surface. Thus, to exceed 5 mph, for example, a drop height greater than 0.8 ft is required; to exceed 30 mph impact, a drop height greater than 30 ft is required. Using the results cited above:

- LOS for the truck SLS cask would occur at impact speeds of about 0.8 ft (5 mph) for corner impact and about 10 ft (18 mph) for end impact
- LOS for the rail SLS cask would occur at about 0.5 ft (3 mph) for corner impact and about 30 ft (30 mph) for end impact.

Such drop heights could occur in some geologic repository operations area (GROA) handling operations.

However, when the effect of the energy absorption by real targets is considered, much greater impact speeds are required to impose the damage equivalent to impacts on unyielding targets. NUREG/CR-6672 (Ref. D4.1.65) provides a correlation of impact speeds for real versus unyielding target, but provides only bounding values for a large number of cases as presented in Table D3.3-2. Therefore, if LOS occurs at 30 mph for an end drop of a SLS train cask on unyielding surface, a speed of greater than 150 mph is required for an impact on concrete. This impact speed would require a drop of over 500 ft. Such drop heights cannot be achieved in repository handling.

Some of the LOS cases, including corner drops of truck and rail SLS casks, appear to result in LOS for impact speeds less than 10 mph. If the corner drops are onto concrete, a speed of 2 to 3 times the threshold speed for LOS for impact on an unyielding target. This implies a threshold impact speed of 20 to 30 mph for a corner drop onto concrete. The corresponding drop height is 13 feet to 30 feet. Such drops could occur in event sequences for repository handling.

Table D3.3-1. Drop Height to Reach a Given Impact Speed

Impact Speed, mph	Equivalent Drop Height, ft
2	0.1
5	0.8
10	3.3
20	13.4
30	30.1
40	53.4
50	83.5
60	120.2
70	163.7
80	213.8
90	270.6
100	334.0
110	404.2
120	481.0

Source: Original

Table D3.3-2. Impact Speeds on Real Target for Equivalent Damage for Unyielding Targets

Cask Type	Real Target Type	Impact Type\Orientation w/o Impact Limiters	Impact Speed, mph			
			30	60	90	120
Rail SLS	Soil	End	>>150	>>150	>>150	>>150
		Side	72	>150	>>150	>>150
		Corner	68	133	>150	>150
	Concrete slab	End	>150	>>150	>>150	>>150
		Side	85	>150	>>150	>>150
		Corner	>>150	>>150	>>150	>>150
Truck SLS	Soil	End	>150	>>150	>>150	>>150
		Side	70	>150	>>150	>>150
		Corner	61	>150	>>150	>>150
	Concrete slab	End	123	180	>>150	>>150
		Side	35	86	135	>150
		Corner	56	123	>150	>>150

NOTE: mph = miles per hour; SLS = steel-lead-steel.

Source: Based on NUREG/CR-6672 (Ref. D4.1.65, Tables 5.10 and 5.12)

D3.4 PROBABILITY OF LOSS OF SHIELDING

NUREG/CR-6672 (Ref. D4.1.65) develops probabilities for LOS in transportation accidents. The probability of LOS uses event tree analysis with split fractions for various types of transportation accidents and frequencies based on accident rates per mile of travel for cask-bearing truck trailers or rail cars. The results of probability analyses of LOS as derived in NUREG/CR-6672 (Ref. D4.1.65) do not have any direct relevance to event sequences for waste handling operations. However, the basic approach that breaks down the overall probability of an event sequence involving LOS into conditional probabilities for occurrence of various physical conditions that lead to LOS can be adapted for PCSA.

The vulnerability to LOS for repository event sequences varies with the container type:

1. Concrete overpack with no containment boundary (aging overpack)
2. Sandwich type with steel containment boundary and lead in the annulus between the steel shells (transportation cask).
3. All other casks including monolithic steel casks or casks with layers of steel or steel and depleted uranium (transportation cask, STC).

Concrete Overpacks

Aging overpacks provide shielding but not containment. They are used within the GROA to transport DPCs and TAD canisters between buildings and to and from the aging pads. The event sequences that involve both are of the form shown in Figure D3.4-1 below.

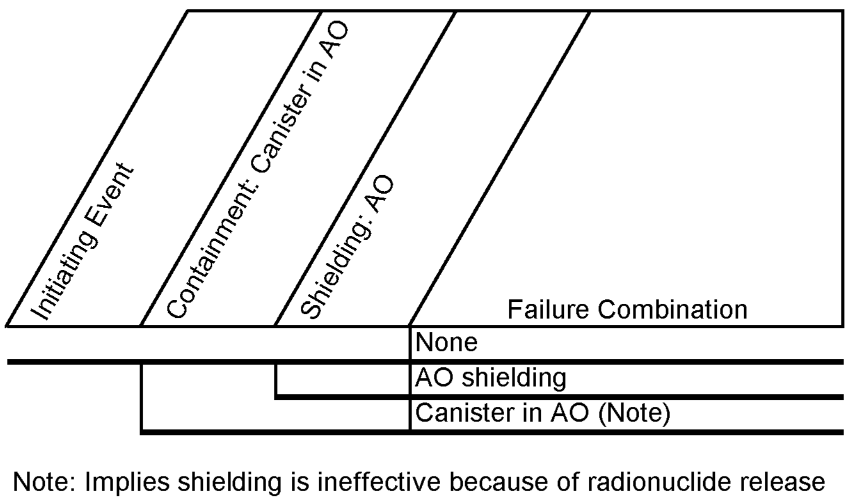

NOTE: AO = aging overpack.

Source: Original

Figure D3.4-1. Summary Event Tree Showing Model Logic for Canisters and Aging Overpacks

A site transporter transports aging overpacks with canisters within the GROA. The transporter is designed for a maximum speed of 2.5 mph (Ref. D4.1.18, Sections 3.2.1 and 3.2.4) and will elevate the aging overpack no more than 3 feet from the ground (equipment limit is 12 inches (Ref. D4.1.18, Section 2.2, item 9)), additional two feet is allowed for potential drop off edge of aging pad). Expanding the probability of success (no breach) of a canister within an aging overpack yields:

$$p_{AO}(C) = p_{AO}(C \mid O) p_{AO}(O) + p_{AO}(C \mid \overline{O}) p_{AO}(\overline{O}), \qquad \text{(Eq. D-26)}$$

where

$p_{AO}(C)$ = probability of canister success within an AO.

$p_{AO}(C \mid O)$ = probability of canister success given AO shielding does not fail.

$p_{AO}(O)$ = probability that AO shielding does not fail.

$p_{AO}(C \mid \overline{O})$ = probability of canister success given AO shielding fails.

$p_{AO}(\overline{O})$ = probability that AO shielding fails.

The inner and outer steel lined 3 foot concrete aging overpack is much more robust against impact loads than a DPC. Therefore, if the overpack fails, it is much more likely that the canister will breach. This yields: $\mathrm{p_{AO}(C \mid O) >> p_{AO}(C \mid \overline{O})}$. Furthermore, the probability of aging overpack breach is much less than probability of aging overpack success at the above drop and speed conditions. Therefore: $\mathrm{p_{AO}(O) >> p_{AO}(\overline{O})}$. The second term on the right hand side of Equation D-26 is much less than the first term and need not be considered further in this analysis.

This leaves

$$p_{AO}(C) \cong p_{AO}(C \mid O) p_{AO}(O) \qquad \text{(Eq. D-27)}$$

Note that

$p_{AO}(C) = 1 - p_{AO}(\overline{C})$ and $p_{AO}(O) = 1 - p_{AO}(\overline{O})$ and

$$p_{AO}(C \mid O) = 1 - p_{AO}(\overline{C} \mid O) \qquad \text{(Eq. D-28)}$$

Substituting Equations D-28 into D-27 and rearranging yields:

$$\mathrm{p_{AO}(\overline{O}) \cong 1 - \frac{1 - p_{AO}(\overline{C})}{1 - p_{AO}(\overline{C} \mid O)}} \qquad \text{(Eq. D-29)}$$

LLNL has developed a mean probability of failure for a canister within an aging overpack, $p_{AO}(\overline{C})$, for a 3-foot drop onto a rigid surface with an initial velocity of 2.5 mph (Ref. D4.1.27).

This analysis uses a conservative value of 1E-05 relative to the 1E-08 value in the referenced LLNL report. The probability of canister failure given the aging overpack does not fail, $p_{AO}(\overline{C} \mid O)$, must be less than the overall probability of canister failure within an aging overpack, $p_{AO}(\overline{C})$. It is, therefore, reasonable to use a range of values of 1E-06 to 1E-05 for this, both of which are conservative relative to the value in the reference. The LLNL (Ref. D4.1.27) value, itself, has a conservative element in that it analyzes impact onto a rigid surface. The more realistic concrete surface would have a lower canister failure probability. Using the average between 1E-06 and 1E-05 of 5E-06 for $p_{AO}(\overline{C} \mid O)$ and also substituting the aforementioned value for $p_{AO}(\overline{C})$ into Equation D-29, there obtains:

$$p_{AO}(\overline{O}) \cong 1 - \frac{1 - p_{AO}(\overline{C})}{1 - p_{AO}(\overline{C} \mid O)} = 1 - \frac{1 - 10^{-5}}{1 - 5 \times 10^{-6}} = 5 \times 10^{-6} \qquad \text{(Eq. D-30)}$$

Steel/Lead/Steel Sandwich-Type Casks

For these sandwich-type casks, the probability of LOS due to lead slumping can be estimated from results of transportation cask studies that can be coupled to event sequence probability analysis and insights from the passive failure analyses. Since the speed of transport of transportation casks to, and within, the processing facilities is limited to a few mph, it is judged that LOS of SLS casks (and the other types) may be screened out from collision scenarios. However, LOS for SLS casks due to drops cannot be ruled out, if SLS casks are processed in the repository.

For SLS casks, the probability of LOS is derived from the probability that the drop height or impact speed exceeds the threshold at which lead shielding may slump. For all cask types, the probability of LOS is derived from the probability that the drop height or impact speed exceeds the threshold at which cask closure and/or seals fail in such a way to permit to permit direct streaming. A simplified conservative approach to estimating the probability of LOS due to lead slumping resulting from a drop of an SLS cask is summarized in the next section.

The PCSA considers drop and collision event sequences of transportation casks. Should a canister rupture occur, the analysis conservatively models the shielding as also lost. In such event sequences the probability of loss of shielding is taken to be 1.0 given canister rupture. This applies to all types of casks.

Event sequences also include LOS without canister rupture. That is, the drop or collision was not severe enough to cause a rupture but a LOS is possible in some casks. Such an event sequence can not occur in the steel/depleted uranium truck casks. The loss of shielding associated with streaming through the head of steel monolith rail casks is due to structural failure of the casks. The probability of this is estimated by taking the breach/rupture probability of a steel monolith transportation cask at the weakest location and applying it as a head rupture probability.

Collisions of casks will occur at less than 5 mph. Drops can occur as high as 30 feet. Drops may be at any orientation: side, bottom, and end. A conservative approach to estimation of the probability of SLS LOS is to use the information associated with end drops, which can cause bulging of the steel containment that allows the lead to collect towards one end. Although the corner impact can cause greater strain in the steel containment, it does not cause the spreading that increases collection of the lead at one end. All surfaces in the repository upon which a transportation cask can be dropped (concrete or soil) are concrete or softer. Therefore, the concrete related drop height vs. LOS information may be accurately used.

An impact of at least 123 mph against a real surface such as concrete or soil is required in order to cause the same damage as an impact of 30 mph against an unyielding surface (Table D3.3-2). The vast majority of casks are to be delivered to the repository by rail. The maximum strain due to an end impact of 30 mph against an unyielding surface, or 123 mph against a real surface, is about 3.9% for a truck cask (greater than the 1.9% strain for a rail cask) (Table D3.2-1). Noting in Figure D3.2-3 that the amount of strain is roughly linear with the impact velocity, a velocity of 63 mph is estimated to correspond to the strain of 2% indicative of S3 damage and lead slumping. A 63 mph collision, equivalent to a 133-foot drop, is the threshold for causing enough damage to indicate potential loss of shielding due to lead slumping.

In order to develop fragility over height, the available information described herein indicates that an estimate of a median threshold for a failure drop height is 133 feet. This would yield 2% strain. A coefficient variation (the ratio of standard deviation to the median) is 0.1. This is an estimate derived from the distribution of capacity associated with the tensile strength elongation data described in Section D1.1. The probability of LOS due to lead slumping resulting from a 15-foot vertical drop would be less than 1×10^{-8}, given the drop event. For a 30-foot drop resulting from a 2-blocking event, the computed failure probability based on the 133-foot median drop height is also less than 1×10^{-8}. LOS due to lead slumping applies only to those casks using lead for shielding but the PCSA applied this analysis to all casks. A conservative value of 1×10^{-5} is used to be consistent with the probabilities based on the LLNL (Ref. D4.1.27) results.

Results are shown in Tables D3.4-1.

Table D3.4-1. Probabilities of Degradation or Loss of Shielding

Description	Probability	Note
Sealed transportation cask and shielded transfer casks shielding degradation after structural challenge	1×10^{-5}	Section D3.4
Aging overpack shielding loss after structural challenge	5×10^{-6}	Section D3.4
CTM shielding loss after structural challenge	0	Structural challenge sufficiently mild to leave the shielding function intact[a]
WPTT shielding loss after structural challenge	0	Structural challenge sufficiently mild to leave the shielding function intact[a]
TEV shielding loss (shield end)	0	Structural challenge sufficiently mild to leave the shielding function intact[a]
Shielding loss by fire for waste forms in transportation casks or shielded transfer casks	1	Lead shielding could potentially expand and degrade. This probability is conservatively applied to transportation casks and STCs that do not use lead for shielding
Shielding loss by fire of aging overpacks, CTM shield bell, and WPTT shielding	0	Type of concrete used for aging overpacks is not sensitive to spallation; Uranium used in CTM shield bell and WPTT shielding does not lose its shielding function as a result of fire

NOTE: [a] In the event sequence diagrams of the PCSA, the shielding function for the CTM, WPTT and TEV is queried for the challenges that do not lead to a radioactive release. Such challenges, which were not sufficiently severe to cause a breach of containment of the waste form container, are also deemed mild enough to leave the shielding function of the CTM, WPTT and TEV intact.

CTM = canister transfer machine; STC = shielded transfer cask; TEV=transport and emplacement vehicle; WPTT = waste package transfer trolley.

Source: Original

All Other Cask Types

For all other cask types, the results of the transportation cask study indicate that the only mechanism for LOS is streaming via closure failures and closure geometry changes. Therefore, the probability of LOS can be equated to the probability of rupture/breach of such casks.

D4 REFERENCES

D4.1 DESIGN INPUTS

The PCSA is based on a snapshot of the design. The reference design documents are appropriately documented as design inputs in this section. Since the safety analysis is based on a snapshot of the design, referencing subsequent revisions to the design documents (as described in EG-PRO-3DP-G04B-00037, *Calculations and Analyses* (Ref. 2.1.1, Section 3.2.2.F)) that implement PCSA requirements flowing from the safety analysis would not be appropriate for the purpose of this document. There are no superseded or cancelled documents associated with the modifications that led to the issuance of this revision. Cancelled or superseded documents associated with the portions of this document for which the snapshot has not yet been updated are designated herein with a dagger (†).

The inputs in this Section noted with an asterisk (*) indicate that they fall into one of the designated categories described in Section 4.1, relative to suitability for intended use.

D4.1.1 *Allegheny Ludlum 2006. "Technical Data Blue Sheet, Stainless Steels Chromium-Nickel-Molybdenum, Types 316 (S31600), 316L (S31603), 317 (S31700), 317L (S31703)." Technical Data Blue Sheet. Brackenridge, Pennsylvania: Allegheny Ludlum. TIC: 259471. LC Call Number: TA 486 .A4 2006.

D4.1.2 *A.M. Birk Engineering 2005. *Tank Car Thermal Protection Defect Assessment: Updated Thermal Modelling with Results of Fire Testing*. TP 14367E. Ontario, Canada: Transportation Development Centre of Transport Canada. ACC: MOL.20071113.0095.

D4.1.3 *ASM (American Society for Metals) 1961. "Properties and Selection of Metals." Volume 1 of *Metals Handbook*. 8th Edition. Lyman, T.; ed. Metals Park, Ohio: American Society for Metals. TIC: 257281. LC Call Number: TA459 .M43 1961 Vol.1.

D4.1.4 *ASM 1976. *Source Book on Stainless Steels*. Metals Park, Ohio: American Society for Metals. TIC: 259927. LC Call Number: TA479 .S7 S64 1976.

D4.1.5 *ASME (American Society of Mechanical Engineers) 2001. *2001 ASME Boiler and Pressure Vessel Code (includes 2002 addenda)*. New York, New York: American Society of Mechanical Engineers. TIC: 251425.

D4.1.6 *ASME 2004. *2004 ASME Boiler and Pressure Vessel Code*. 2004 Edition. New York, New York: American Society of Mechanical Engineers. TIC: 256479.

D4.1.7 *ASTM (American Society for Testing and Materials) G 1-03. 2003. *Standard Practice for Preparing, Cleaning, and Evaluating Corrosion Test Specimens*. West Conshohocken, Pennsylvania: American Society for Testing and Materials. TIC: 259413.

D4.1.8 *Avallone, E.A. and Baumeister, T., III, eds. 1987. *Marks' Standard Handbook for Mechanical Engineers.* 9th Edition. New York, New York: McGraw-Hill. TIC: 206891. ISBN: 0-07-004127-X.

D4.1.9 *BNFL Fuel Solutions 2003. *FuelSolutions™ TS125 Transportation Cask Safety Analysis Report, Revision 5.* Document No. WSNF-120. Docket No. 71-9276. Campbell, California: BNFL Fuel Solutions. TIC: 257634.

D4.1.10 Not Used.

D4.1.11 BSC (Bechtel SAIC Company) 2006. *CRCF, IHF, RF, and WHF Canister Transfer Machine Mechanical Equipment Envelope.* 000-MJ0-HTC0-00201-000 REV 00A. Las Vegas, Nevada: Bechtel SAIC Company. ACC: ENG.20061120.0011.

D4.1.12 †BSC 2007. *Mechanical Handling Design Report: Waste Package Transport and Emplacement Vehicle.* 000-30R-HE00-00200-000 REV 001. Las Vegas, Nevada: Bechtel SAIC Company. ACC: ENG.20071205.0002.

D4.1.13 BSC 2007. *5-DHLW/DOE SNF - Long Co-Disposal Waste Package Configuration.* 000-MW0-DS00-00203-000 REV 00C. Las Vegas, Nevada: Bechtel SAIC Company. ACC: ENG.20070719.0007.

D4.1.14 BSC 2007. *Aging Facility Vertical DPC Aging Overpack Mechanical Equipment Envelope Sheet 1 of 2.* 170-MJ0-HAC0-00201-000 REV 00B. Las Vegas, Nevada: Bechtel SAIC Company. ACC: ENG.20070928.0032.

D4.1.15 †BSC 2007. *Basis of Design for the TAD Canister-Based Repository Design Concept.* 000-3DR-MGR0-00300-000-001. Las Vegas, Nevada: Bechtel SAIC Company. ACC: ENG.20071002.0042.

D4.1.16 *BSC 2007. *Discipline Design Guide and Standards for Surface Facilities HVAC Systems.* 000-3DG-GEHV-00100-000-00A. Las Vegas, Nevada: Bechtel SAIC Company. ACC: ENG.20070514.0007.

D4.1.17 BSC 2007. *Leak Path Factors for Radionuclide Releases from Breached Confinement Barriers and Confinement Areas.* 000-00C-MGR0-01500-000-00A. Las Vegas, Nevada: Bechtel SAIC Company. ACC: ENG.20071018.0002.

D4.1.18 †BSC 2007. *Mechanical Handling Design Report - Site Transporter.* 170-30R-HAT0-00100-000-000. Las Vegas, Nevada: Bechtel SAIC Company. ACC: ENG.20071217.0015.

D4.1.19 BSC 2007. *Naval Long Oblique Impact Inside TEV.* 000-00C-DNF0-01200-000-00A. Las Vegas, Nevada: Bechtel SAIC Company. ACC: ENG.20070806.0016.

D4.1.20 BSC 2007. *Naval Long Waste Package Vertical Impact on Emplacement Pallet and Invert.* 000-00C-DNF0-00100-000-00C. Las Vegas, Nevada: Bechtel SAIC Company. ACC: ENG.20071017.0001.

D4.1.21 BSC 2007. *Probabilistic Characterization of Preclosure Rockfalls in Emplacement Drifts.* 800-00C-MGR0-00300-000-00A. Las Vegas, Nevada: Bechtel SAIC Company. ACC: ENG.20070329.0009.

D4.1.22 BSC 2007. *TAD Waste Package Configuration.* 000-MW0-DSC0-00101-000 REV 00B. Las Vegas, Nevada: Bechtel SAIC Company. ACC: ENG.20070301.0010.

D4.1.23 BSC 2007. *TAD Waste Package Configuration.* 000-MW0-DSC0-00102-000 REV 00B. Las Vegas, Nevada: Bechtel SAIC Company. ACC: ENG.20070301.0011.

D4.1.24 BSC 2007. *TAD Waste Package Configuration.* 000-MW0-DSC0-00103-000 REV 00B. Las Vegas, Nevada: Bechtel SAIC Company. ACC: ENG.20070301.0012.

D4.1.25 BSC 2007. *Thermal Responses of TAD and 5-DHLW/DOE SNF Waste Packages to a Hypothetical Fire Accident.* 000-00C-WIS0-02900-000-00A. Las Vegas, Nevada: Bechtel SAIC Company. ACC: ENG.20070220.0008.

D4.1.26 BSC 2007. *Waste Package Capability Analysis for Nonlithophysal Rock Impacts.* 000-00C-MGR0-04500-000-00A. Las Vegas, Nevada: Bechtel SAIC Company. ACC: ENG.20071113.0017.

D4.1.27 BSC 2008. *Seismic and Structural Container Analyses for the PCSA*. 000-PSA-MGR0-02100-000-00A. Las Vegas, Nevada: Bechtel SAIC Company. ACC: ENG.20080220.0003.

D4.1.28 †DOE (U.S. Department of Energy) 2007. *Transportation, Aging and Disposal Canister System Performance Specification.* WMO-TADCS-000001, Rev. 0. Washington, D.C.: U.S. Department of Energy, Office of Civilian Radioactive Waste Management. ACC: DOC.20070614.0007.

D4.1.29 †DOE 2007. *Quality Assurance Requirements and Description.* DOE/RW-0333P, Rev. 19. Washington, D.C.: U.S. Department of Energy, Office of Civilian Radioactive Waste Management. ACC: DOC.20070717.0006. (DIRS 182051)

D4.1.30 *English, G.W.; Moynihan, T.W.; Worswick, M.J.; Birk, A.M. 1999. *A Railroad Industry Critique of the Model Study.* 96-025-TSD. Kingston, Ontario, Canada: TranSys Research. TIC: 260032.

D4.1.31 *Evans, D.D. 1993. "Sprinkler Fire Suppression Algorithm for HAZARD." *Fire Research and Safety, 12th Joint Panel Meeting, October 27-November 2, 1992, Tsukuba, Japan.* Pages 114-120. Tsukuba, Japan: Building Research Institute and Fire Research Institute. ACC: MOL.20071114.0163.

D4.1.32 *Fischer, L.E.; Chou, C.K.; Gerhard, M.A.; Kimura, C.Y.; Martin, R.W.; Mensing, R.W.; Mount, M.E.; and Witte, M.C. 1987. *Shipping Container Response to Severe*

Highway and Railway Accident Conditions. NUREG/CR-4829. Two volumes. Washington, D.C.: U.S. Nuclear Regulatory Commission. ACC: NNA.19900827.0230; NNA.19900827.0231.

D4.1.33 *Friedrich, T. and Schellhaas, H. 1998. "Computation of the percentage points and the power for the two-sided Kolmogorov-Smirnov one sample test." *Statistical Papers 39,* 361-375. New York, New York: Springer-Verlag. TIC: 260013.

D4.1.34 *General Atomics 1995. *GA-9 Legal Weight Truck From-Reactor Spent Fuel Shipping Cask, Final Design Report (FDR).* 910354 N/C. San Diego, California: General Atomic. ACC: MOV.20000106.0003.

D4.1.35 *Haynes International 1990. Reliability and Longevity of Furnace Components as Influenced by Alloy of Construction. H-3124. Kokomo, Indiana: Haynes International. TIC: 256362.

D4.1.36 *Haynes International 1997. Hastelloy C-22 Alloy. Kokomo, Indiana: Haynes International. TIC: 238121.

D4.1.37 *Hertz, K.D. 2003. "Limits of Spalling of Fire-Exposed Concrete." *Fire Safety Journal, 38,* 103-116. New York, New York: Elsevier. TIC: 259993.

D4.1.38 *Holtec International 2003. *Storage, Transport, and Repository Cask Systems, (Hi-Star Cask System) Safety Analysis Report, 10 CFR 71, Docket 71-9261.* HI-951251, Rev. 10. Marlton, New Jersey: Holtec International. ACC: MOL.20050119.0271.

D4.1.39 *Holtec International 2005. *Final Safety Analysis Report for the HI-STORM 100 Cask System.* USNRC Docket No.: 72-1014. Holtec Report No.: HI-2002444. Marlton, New Jersey: Holtec International. TIC: 258829.

D4.1.40 *NIST (National Institute of Standards and Technology) 2004. "Concrete, Ordinary." *Table 4. X-Ray Mass Attenuation Coefficients.* Gaithersburg, Maryland: National Institute of Standards and Technology. Accessed March 3, 2008.
ACC: MOL.20080303.0046.
URL: http://physics.nist.gov/PhysRefData/XrayMassCoef/tab4.html .

D4.1.41 *Incropera, F.P. and DeWitt, D.P. 1996. *Introduction to Heat Transfer*. 3rd Edition. New York, New York: John Wiley and Sons. TIC: 241057. ISBN: 0-471-30458-1.

D4.1.42 Not used.

D4.1.43 *Kodur, V.K.R.; Wang, T.C.; and Cheng, F.P. 2004. "Predicting the Fire Resistance Behaviour of High Strength Concrete Columns." *Cement & Concrete Composites, 26,* 141-153. New York, New York: Elsevier. TIC: 259996.

D4.1.44 *Larson, F.R. and Miller, J. 1952. "A Time-Temperature Relationship for Rupture and Creep Stresses." *Transactions of the American Society of Mechanical Engineers, 74,* 765-775. New York, New York: American Society of Mechanical Engineers. TIC: 259911.

D4.1.45 †Lide, D.R., ed. 1995. *CRC Handbook of Chemistry and Physics.* 76th Edition. Boca Raton, Florida: CRC Press. TIC: 216194. ISBN: 0-84930476-8.

D4.1.46 *Majumdar, S.; Shack, W.J.; Diercks, D.R.; Mruk, K.; Franklin, J.; and Knoblich, L. 1998. *Failure Behavior of Internally Pressurized Flawed and Unflawed Steam Generator Tubing at High Temperatures – Experiments and Comparisons with Model Predictions.* NUREG/CR-6575. Washington, D.C.: U.S. Nuclear Regulatory Commission. ACC: MOL.20071106.0053.

D4.1.47 *Mason, M. 2001. "NUHOMS-MP197 Transport Packaging Safety Analysis Report." Letter from M. Mason (Transnuclear) to E.W. Brach (NRC), May 2, 2001, E-21135, with enclosures. TIC: 255258.

D4.1.48 *Morris Material Handling 2008. *Mechanical Handling Design Report - Canister Transfer Machine.* V0-CY05-QHC4-00459-00018-001-004. Morris Material Handling. ACC: ENG.20080121.0010.

D4.1.49 †*NAC (Nuclear Assurance Corporation) 2000. *Safety Analysis Report for the NAC Legal Weight Truck Cask.* Revision 29. Docket No. 71-9225. T-88004. Norcross, Georgia: Nuclear Assurance Corporation International. ACC: MOL.20070927.0003.

D4.1.50 *NAC 2004. "NAC-STC NAC Storage Transport Cask, Revision 15." Volume 1 of *Safety Analysis Report.* Docket No. 71-9235. Norcross, Georgia: NAC International. TIC: 257644.

D4.1.51 *Nakos, J.T. 2005. *Uncertainty Analysis of Steady State Incident Heat Flux Measurements in Hydrocarbon Fuel Fires.* SAND2005-7144. Albuquerque, New Mexico: Sandia National Laboratories. ACC: MOL.20071106.0054.

D4.1.52 *Nowlen, S.P. 1986. *Heat and Mass Release for Some Transient Fuel Source Fires: A Test Report.* NUREG/CR-4680. Washington, D.C.: U.S. Nuclear Regulatory Commission. ACC: MOL.20071113.0099.

D4.1.53 *Nowlen, S.P. 1987. *Quantitative Data on the Fire Behavior of Combustible Materials Found in Nuclear Power Plants: A Literature Review.* NUREG/CR-4679. Washington, D.C.: U.S. Nuclear Regulatory Commission. ACC: MOL.20071113.0100.

D4.1.54 *NRC (U.S. Nuclear Regulatory Commission) 1997. *Standard Review Plan for Dry Cask Storage Systems.* NUREG-1536. Washington, D.C.: U.S. Nuclear Regulatory Commission. ACC: MOL.20010724.0307.

D4.1.55 *NRC 2003. *Interim Staff Guidance - 18. The Design/Qualification of Final Closure Welds on Austenitic Stainless Steel Canisters as Confinement Boundary for Spent Fuel*

Storage and Containment Boundary for Spent Fuel Transportation. ISG-18. Washington, D.C.: U.S. Nuclear Regulatory Commission. TIC: 254660.

D4.1.56 *NRC 2007. *Interim Staff Guidance HLWRS-ISG-02, Preclosure Safety Analysis - Level of Information and Reliability Estimation.* HLWRS-ISG-02. Washington, D.C.: U.S. Nuclear Regulatory Commission. ACC: MOL.20071018.0240.

D4.1.57 *Quintiere, J.G. 1998. *Principles of Fire Behavior.* Albany, New York: Delmar Publishers. TIC: 251255. ISBN: 0-8273-7732-0.

D4.1.58 *Rieth, M.; Falkenstein, A.; Graf, P.; Heger, S.; Jäntsch, U.; Klimiankou, M.; Materna-Morris, E.; and Zimmermann, H. 2004. *Creep of the Austenitic Steel AISI 316L(N), Experiments and Models.* FZKA 7065. Karlsruhe, Germany: Forschungszentrum Karlsruhe GmbH. TIC: 259943.

D4.1.59 *Sasikala, G.; Mathew, M.D.; Bhanu Sankara Rao, K.; and Mannan, S.L. 1997. "Assessment of Creep Behaviour of Austenitic Stainless Steel Welds." *Creep-Fatigue Damage Rules for Advanced Fast Reactor Design, Proceedings of a Technical Committee Meeting, Manchester, United Kingdom, 11-13 June 1996.* IAEA-TECDOC-993. Pages 219-227. Vienna, Austria: International Atomic Energy Agency. TIC: 259880.

D4.1.60 *Savolainen, K.;Mononen, J.; Ilola, R.; Hanninen, H. 2005. *Materials Selection for High Temperature Applications.* TKK-MTR-4/05. Espoo, Finland: Otamedia Oy. TIC: 259896. ISBN: 951-22-7892-8.

D4.1.61 †*Society of Fire Protection Engineering (SFPE) 1988. *The SFPE Handbook of Fire Protection Engineering, Society of Fire Protection Engineers.* Edition 1. Quincy, Massachusetts: National Fire Protection Association. TIC: 101351. ISBN: 0-87765-353-4 .

D4.1.62 *Shapiro, S. S. and Wilk, M. B. 1965. "An analysis of variance test for normality (complete samples)", *Biometrika*, 52 (3 - 4), pages 591-611. Cary, North Carolina: Oxford University Press. TIC: 259992.

D4.1.63 *Siegel, R. and Howell, J.R. 1992. *Thermal Radiation Heat Transfer.* 3rd Edition. Washington, D.C.: Taylor & Francis. TIC: 236759. ISBN: 0-89116-271-2. (Radiation view factors also available online at: http://www.me.utexas.edu/~howell/index.html.)

D4.1.64 *Snow, S.D. 2007. *Structural Analysis Results of the DOE SNF Canisters Subjected to the 23-Foot Vertical Repository Drop Event to Support Probabilistic Risk Evaluations.* EDF-NSNF-085, Rev. 0. Idaho Falls, Idaho: Idaho National Laboratory. ACC: MOL.20080206.0062.

D4.1.65 *Sprung, J.L.; Ammerman, D.J.; Breivik, N.L.; Dukart, R.J.; Kanipe, F.L.; Koski, J.A.; Mills, G.S.; Neuhauser, K.S.; Radloff, H.D.; Weiner, R.F.; and Yoshimura, H.R. 2000. *Reexamination of Spent Fuel Shipment Risk Estimates.* NUREG/CR-6672. Two volumes. Washington, D.C.: U.S. Nuclear Regulatory Commission. ACC: MOL.20001010.0217.

D4.1.66 *Transnuclear 2001. *TN-68 Transport Packaging Safety Analysis Report, Revision 4.* Hawthorne, New York: Transnuclear. TIC: 254025. D4.1.67 Snow, S.D. and Morton, D.K. 2007. Qualitative Analysis of the Standardized DOE SNF Canister for Specific Canister-on-Canister Drop Events at the Repository. EDF-NSNF-087, Rev. 0. [Idaho Falls, Idaho: Idaho National Laboratory]. ACC: MOL.20080206.0063. (DIRS 184973)

D4.2 DESIGN CONSTRAINTS

D4.2.1 †10 CFR 20. 2007. Energy: Standards for Protection Against Radiation. Internet Accessible

D4.2.2 †10 CFR 71. 2007. Energy: Packaging and Transportation of Radioactive Material. ACC: MOL.20070829.0114.

INTENTIONALLY LEFT BLANK

ATTACHMENT E
HUMAN RELIABILITY ANALYSIS